Received: 24 January 2022 | Revised: 26 February 2024 | Accepted: 29 March 2024

DOI: 10.1002/esp.5847

RESEARCH ARTICLE

ESPL WILEY

Fluviomorphic trajectories for dryland ephemeral stream channels following extreme flash floods

Eliisa Lotsari[1,2,3] | P. Kyle House[4] | Petteri Alho[3,5] | Victor R. Baker[6]

[1]Water and Environmental Engineering, Department of Built Environment, Aalto University, Aalto, Finland

[2]Department of Geographical and Historical Studies, University of Eastern Finland, Joensuu, Finland

[3]Department of Geography and Geology, University of Turku, Turku, Finland

[4]US Geological Survey (USGS), Flagstaff, Arizona, USA

[5]Finnish Geospatial Research Institute FGI, National Land Survey of Finland, Espoo, Finland

[6]Department of Hydrology and Atmospheric Sciences, University of Arizona, Tucson, Arizona, USA

Correspondence
Eliisa Lotsari, Water and Environmental Engineering, Department of Built Environment, Aalto University, PO Box 15200, Tietotie 1E, FI-00076 Aalto, Finland.
Email: eliisa.s.lotsari@aalto.fi

Funding information
Academy of Finland, Grant/Award Numbers: 338480, 267345, 136234; Turun Yliopisto

Abstract

Ephemeral alluvial streams pose globally significant flood hazards to human habitation in drylands, but sparse data for these regions limit understanding of the character and impacts of extreme flooding. In this study, we document decadal changes in dryland ephemeral channel patterns at two sites in the lower Colorado River Basin (southwestern United States) that were ravaged by extraordinary flash floods in the 1970s: Bronco Creek, Arizona (1971), and Eldorado Canyon, Nevada (1974). We refer to these two floods as 'fluviomorphic erasure events', because they produced blank slates for the channels that were gradually moulded by more frequent but much smaller flood events. We studied georectified aerial photos that span ~60 years at each site to show that both study sites recovered to their pre-flood condition after ~25 years. We employ channel network metrics: stream-link area (SLA), geometric braiding index and junction-node density. Each metric decreased during the short-duration extreme flood erasure events. Subsequently, a fluviomorphic trajectory at a decadal tempo returned the channels to pre-flood values. The SLA decreased at rates of 3.6%–4.1% per year in the decade following the floods. The extreme flood events decreased the pre-flood geometric braiding index at the two sites by 56%–68%, and it took 15–24 years for this index to recover to pre-flood values. In contrast, it took 30–35 years for the channels to recover to a uniform pre-flood channel form, as indicated by the spatial distribution of bars and junction nodes. Our results document baseline examples of ephemeral stream channel evolution trajectories, as future climatic change will likely accelerate increases in the magnitudes and frequencies of extreme floods and geomorphic erasure events.

KEYWORDS
bifurcation density, confluence density, drylands, ephemeral streams, flash flooding, fluviomorphic trajectory

1 | INTRODUCTION

1.1 | Extreme flood geomorphology processes in the study area

Analyses of the geomorphic evolution of dryland braided ephemeral channels can reveal trends, magnitudes and rates for key formative processes. Because of rare opportunities for direct study, however, very little research has documented the evolutionary trajectories of streambed recovery following extraordinary flooding. This is the case for many dryland areas, including rugged portions of western Arizona and southern Nevada, USA. Given the prospect for increased future incidences of extreme flooding associated with climate change (Fowler et al., 2021; Hawkins et al., 2015; Intergovernmental Panel on Climate Change [IPCC], 2021; Tousi et al., 2021), our study provides important baseline information for assessing ephemeral stream channel responses to varying flood magnitudes and frequencies.

For ephemeral streams that flow only in direct response to precipitation (Hadley, 1968), the term *flood* represents flow events of all magnitudes, and flash floods are especially common. The channels

conveying these floods can have slopes greater than 0.002 m/m, which is considered steep or high gradient (cf. Jarrett, 1984). Most flash floods in small watersheds in the southwestern United States result from warm-season convective thunderstorms associated with summer monsoonal conditions and rarer moisture plumes from dissipating tropical storms (e.g., House & Hirschboeck, 1997; Mascaro, 2018). The extreme precipitation results in dramatic and damaging floods (e.g., Glancy & Harmsen, 1975; Mascaro, 2018; Sharon, 1972; Smith et al., 2019; Tousi et al., 2021), the magnitude and frequency of which are poorly constrained by inadequate networks of meteorological and hydrological measuring stations. This produces uncertainty for flood risk and vulnerability in desert communities that is compounded by persistent encroachment of human habitation into flood-prone areas (Tellman et al., 2021) and by expected climate-related increases in precipitation intensities and amounts (Fowler et al., 2021; Hawkins et al., 2015; IPCC, 2021; Tousi et al., 2021).

Previous studies in the western United States (Segura et al., 2014; Wolman & Gerson, 1978; Zhang et al., 2012) suggest that a changing climate will lead to more frequent geomorphologically effective flood events that would enhance future erosion rates and landscape change (East & Sankey, 2020). Our study provides a novel approach for overcoming the practical difficulties for adequate monitoring of extreme flood events and associated recovery rates in deserts (e.g., House & Baker, 2001).

1.2 | Desert streams and discontinuous flood geomorphological processes

Small drainage basins with ephemeral streams in the desert of the southwestern United States show a contrast between extreme (potentially catastrophic) and more common flood magnitudes that is much greater than for comparably sized perennial streams in more humid settings (Baker, 1977; Billi et al., 2018; Osterkamp & Friedman, 2000; Smith et al., 2015; Wolman & Gerson, 1978). Moreover, such streams are commonly characterized by spatially and temporally discontinuous fluvial geomorphological processes and patterns (Bull, 1997; Chin & Gregory, 2001; Graf, 1988). Straight braided channels predominate (Billi et al., 2018; Tooth, 2000b), which is attributed to non-cohesive banks and sparse riparian vegetation. Complex interactions among streamflow, sediment transport, slope and patterns of tributary inputs cause variable and discontinuous patterns of downstream channel response (Billi et al., 2018; Tooth, 2000a, 2000b). Channel bars commonly form, and if the slope and the width–depth ratio are sufficiently high, braiding is favoured (Parker, 1976). Intense flash flooding in these dryland ephemeral streams can increase rates of sediment delivery to the main channel and transform it into a shallow braided tract occupying the entire width of the valley floor (e.g., Ortega et al., 2014).

As our study areas demonstrate, extraordinary floods in broad and confined ephemeral streams can create barren, gravelly surfaces composed of large channel and bar structures adjusted to extreme streamflows. We refer to the extreme floods that create up-scaled channel features and denude them of riparian vegetation as 'fluviomorphic erasure events' (FMEEs). The resultant denuded channel with up-scaled streamlined bars and scoured flow paths is likely to impart strong initial control on the routing of subsequent smaller to intermediate-sized floods, which, over time, will evolve to create a more complex interconnected and downscaled braided channel that is adjusted to the lower flow levels.

The occurrence of an FMEE creates an ideal opportunity for examining how an impacted channel will subsequently evolve along a trajectory towards new equilibrium conditions, as influenced by floods much smaller in magnitude than the FMEE. These frequently occurring, small- to moderate-magnitude floods have been shown to influence the evolution of ephemeral channels (Baker, 1977; Hooke & Mant, 2000; Lotsari et al., 2018; Wolman & Miller, 1960), but, in contrast to a rare extreme flood, they are unlikely to erase an evolving braiding structure. Moderate-to-high streamflow peaks can cause substantial incision in ephemeral channels (Hooke & Mant, 2000). Hooke (2015, 2016b) further showed that a variety of morphological responses to large floods (i.e., >50-year recurrence interval) are possible in ephemeral channels depending on a variety of local conditions.

1.3 | Evolution of ungauged ephemeral stream channels following extreme floods

A time series of aerial imagery can reveal temporal changes in ephemeral stream channels affected by flooding (e.g., Graf, 1981). Documentary evidence (photographs, media and technical reports) for the extreme floods in Bronco Creek (Arizona, USA, August 1971) and Eldorado Canyon (Nevada, USA, September 1974) indicates that both streams experienced FMEEs (House & Pearthree, 1995). The image clarity for the flood-induced changes is enhanced by changing distributions of 'fresh' surfaces as well as the coeval obliteration and recovery of desert riparian plants that develop in and near active flow paths. Repeated measurements of various fundamental geometric characteristics of channel network complexity and connectivity in the affected areas can provide a quantitative temporal record of the trajectory of channel network adjustment and evolution following FMEEs.

Temporal changes in ephemeral channel characteristics can be measured with several geometric indices of stream connectivity (e.g., stream-links and the density of bifurcation and confluence nodes). Most examples of aerial time-series analyses of stream channel morphology (East et al., 2017; Howard et al., 1970; Kidová et al., 2016; Ziliani & Surian, 2012) or sediment dynamics (Gray, 2018) are from perennial rivers. However, Kidová et al. (2016) employed a post-flood-period serial geomorphic analysis approach in a study area that included both perennial and episodic (non-perennial) channels, subject to flow once a threshold was crossed. They observed that increases in key channel parameters including total channel length, island number/area, number/density of confluence–diffluence pairs (nodes) and bar area were caused by two floods of moderate magnitude in a 6-year interval. Howard et al. (1970) and East et al. (2017) analysed correlations among braiding characteristics and hydraulic parameters, such as streamflow, to reveal the processes acting on different braided channels. East et al. (2017) found that the Friend and Sinha (1993) braiding index of multi-thread rivers correlated positively with flood peak magnitude.

Despite the increasing numbers of studies of perennial river evolution using historical maps and aerial photographs (e.g., de Musso et al., 2020; East et al., 2017; Kidová et al., 2016), we are not aware of

studies on decadal fluviomorphic trajectories for near-pristine dryland ephemeral streams. Decadal studies for human-impacted ephemeral channels show the importance of considering site-specific conditions as temporal and spatial channel responses vary (Graf, 1981; Jaeger & Wohl, 2011), and that riparian vegetation responds to and interacts with changes in the channel morphology rather than driving channel change (Cadol et al., 2011). It is important to compare these results to those from pristine ephemeral channels whose evolutionary trajectories are influenced by FMEEs.

1.4 | Hypothesis of the research and goals

Based on previous literature, we hypothesize that an FMEE in an ephemeral alluvial channel will create a relatively simple channel network geometry and that the combined effects of subsequent smaller flood events will develop and maintain a more elaborate or complex network. Our study aims to determine the time required for the two study sites, ravaged by FMEEs, to return to their pre-flood conditions. The development and adjustment of braiding are analysed through changes in metrics that represent the degrees of connectivity, complexity and density of the ephemeral channel network in the flood-affected channels. Thus, our study provides a novel approach for advancing understanding of the past and present geomorphic impacts of extreme flood events and associated recovery rates.

2 | STUDY SITES

2.1 | Characteristics of the study reaches and their watersheds

High-gradient ephemeral streams are common in the lower Colorado River Basin in the southwestern United States. Our two study sites, Bronco Creek, Arizona (34.67654° N, 113.59455° W, WGS84), and Eldorado Canyon, Nevada (35.70711° N, 114.71924° W, WGS84), are typical examples (Figure 1). Bronco Creek is a tributary to the Big Sandy River located just south of Wikieup, Arizona, and Eldorado Canyon is a tributary of the Colorado River located east of Nelson, Nevada. Both streams drain watersheds of comparable size (Bronco Creek: 49.2 km^2; Eldorado Canyon: 59.1 km^2). Both sites are located near their contributing watershed's terminal outlet. Bronco Creek terminates as an alluvial fan on the floodplain of the Big Sandy River, and Eldorado Canyon terminates as a fan delta in Lake Mohave, a reservoir on the Colorado River. They have similar desert climates (Costa & Jarrett, 2008), and both drain rugged mountain ranges.

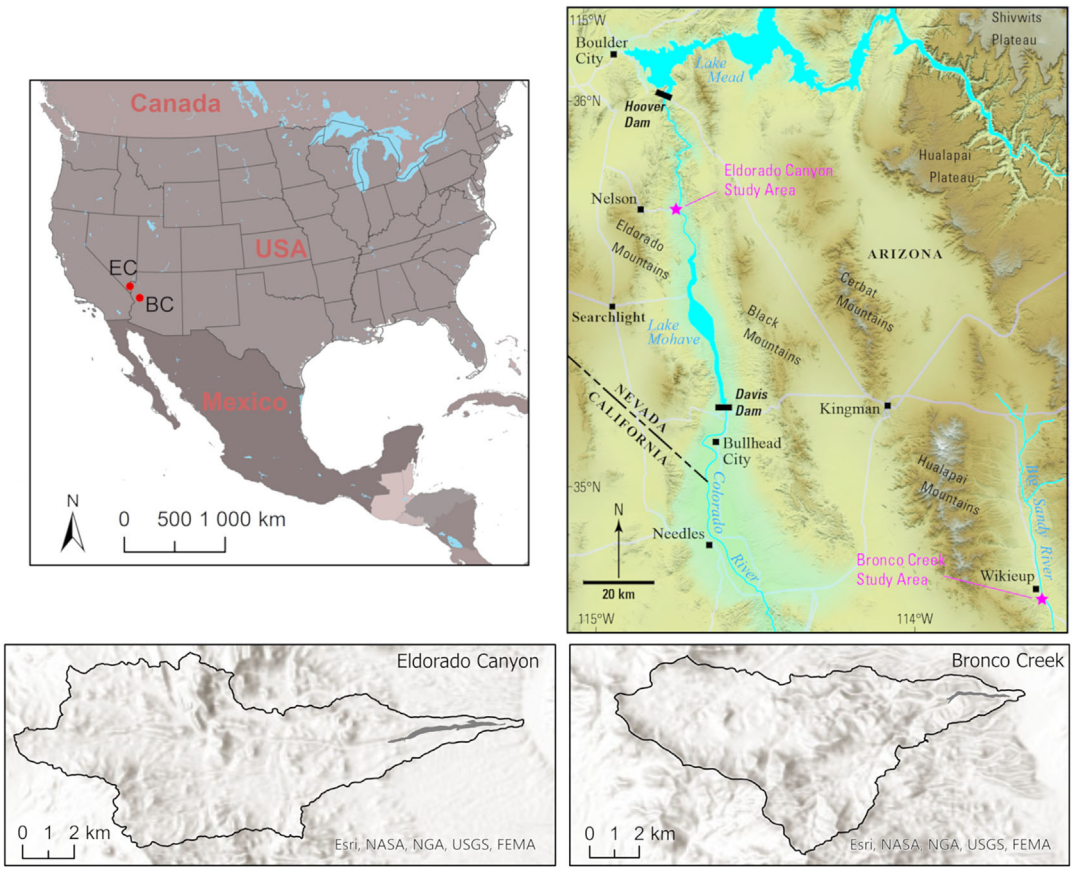

FIGURE 1 The location map for the study sites of Bronco Creek (BC, in Arizona) and Eldorado Canyon (EC, in Nevada). The country borders and water bodies are from USGS, and state borders are from the US Census Bureau/Department of Commerce. The hillshade presented in the two bottom figures is via Esri ArcGIS Pro software (cf. Esri, NASA, USGS and FEMA). The watershed borderlines are from the USGS National Hydrography Dataset (NHD) service (The National Map). The detailed study areas within Bronco Creek and Eldorado Canyon are shown in the two bottom figures with darker grey, which are close to the outlet of the watersheds.

Based on the elevation data (a freely downloadable point cloud based on the 2017 National Agriculture Imagery Program's [NAIP] data from the University of Arizona [https://data.library.arizona.edu/geo/find-data/imagery-lidar] and the primary source at https://catalog.data.gov/dataset/national-agriculture-imagery-program-naip), the upstream end of the Bronco Creek study site is at 644-m elevation, and the downstream end is at 583 m. The longitudinal gradient within the 2217-m-long reach is 0.027 m/m (1.5°). The Eldorado Canyon study site is a 3842-m-long reach extending from 433- to 220-m elevation. This results in a gradient twice that of Bronco Creek (0.056 m/m; 3.2°). Each channel is bounded and confined by relatively high and steeply sloping ridges.

The stream channels of both Bronco Creek and Eldorado Canyon can be classified as braided. According to Miall (1977), 'Braided rivers consist of a series of broad, shallow channels and bars, with elevated areas active only during floods, and dry islands'. This is an apt characterization of the trunk channels of Bronco Creek and Eldorado Canyon. However, their channels are dry very much more frequently than they are wet (Kampf et al., 2016, 2018). The bar and stream-link areas are like braided river morphology, having cobble, gravel and sand-sized particles, as defined by Rinaldi et al. (2016: cf. their fig. 1.13). Their wide, alluvial stream channel beds evolve freely within the channel boundaries, defined by the steep confining hillslopes (cf. Figure 3). No outcroppings of bed-rock that could affect braided channel evolution are within the areas of interest to our study.

In the southwestern United States, winter frontal storms influence cool-season precipitation, and convective storms associated with the North American Monsoon (NAM) are the primary source of warm-season rainfall (Adams & Comrie, 1997; Ziaco et al., 2020). Small watershed flooding in our study area is dominated strongly by convective storms associated with the NAM, but as noted previously, precipitation and streamflow datasets for small and remote desert watersheds are very sparse in the study region and there are no rainfall or streamflow measuring stations within the run-off domain of our study areas.

The Western Regional Climate Center (2011) provides the mean monthly precipitation and average number of days with measurable precipitation in the region (Table 1). Based on those data, the precipitation days per year is 30 for the station closest to Bronco Creek and 26 for the station closest to Eldorado Canyon. Comparatively, the average yearly precipitation is 245 and 196 mm, respectively. The lowest monthly precipitation of 2.286 mm has been in June in Wikieup. Daily precipitation data from these stations are provided by the National Oceanic and Atmospheric Administration (NOAA, 2022: Data for this paper were downloaded in June 2022). According to Kampf et al. (2018), 3–13 mm/h of rain would be required in hyperarid watersheds (such as streams flowing to the Colorado River in AZ and NV) and 7–16 mm/h in semiarid streams for the occurrence of streamflow. Further, Hooke (2016a) showed in Spain that 15–20 mm of rain would be the threshold daily rainfall value for flow. These thresholds have been exceeded annually and in different seasons throughout the study period (Table 1 and Figure 2). Kampf et al. (2016) have observed that in the hyperarid watersheds of the western Sonoran desert area, 36% of the rain events cause flow at 10-cm depth, because much of the rainfall either evaporates or is taken up by plants.

Stream gauge data are not available to reasonably assess the presumable return periods of annual or extreme events in these and

TABLE 1 The mean monthly precipitation and average number of days with measurable precipitation from the town closest to the Bronco Creek (BC) and Eldorado Canyon (EC) study sites (Western Regional Climate Center, 2011: https://wrcc.dri.edu/Climate/comp_tables_states_west.php).

Site	Data	J	F	M	A	M	J	J	A	S	O	N	D	Year
Mean monthly precipitation (mm)														
Wikieup (BC)	1948–2010	36.576	44.958	25.654	10.16	3.81	2.286	22.352	34.798	20.574	16.764	19.05	22.86	244.602
Searchlight (EC)	1914–2010	23.876	24.638	19.812	10.16	5.08	2.794	23.114	27.686	14.986	13.208	10.922	19.304	195.58
Average number of days with measurable precipitation														
Wikieup (BC)	1948–2010	4	3	4	2	1	0	3	4	2	2	2	3	30
Searchlight (EC)	1914–2010	3	3	3	2	1	1	3	3	2	2	2	3	26

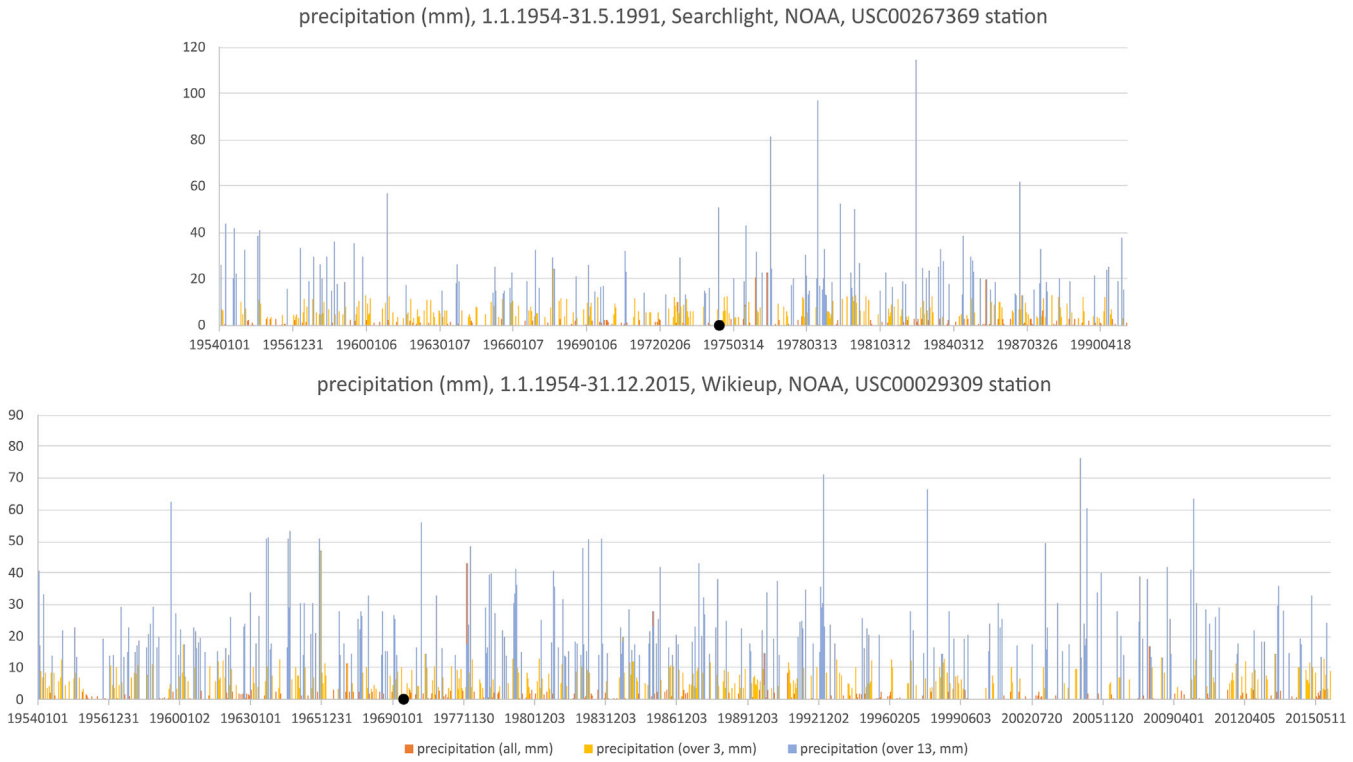

FIGURE 2 The daily precipitation data from Wikieup 1.1.1954–31.12.2015 and Searchlight 1.1.1954–31.5.1991 (Oceanic & Administration, 2022). The Wikieup station is 3.7 km away (straight line) from Bronco Creek's outlet area, and Searchlight is located 33 km (straight line) to the southwest from the outlet of Eldorado Canyon. The timing of the large floods is marked with a black dot on the *x*-axis of both data series. There were no data values since 1991 from the Searchlight station. Note also that there had been a data gap between 31.5.1969 and 1.5.1975 in Bronco Creek, which is exactly when the large flood had taken place (see the location of the black dot). The precipitation has been classified as 'all data', and the thresholds of 3 and 13 mm defined by Kampf et al. (2018) as the requirements for streamflow generation in hyperarid watersheds in the Colorado River Basin (Arizona).

similar systems in the region. The US Geological Survey (USGS) provides a web service that allows users to select a watershed for which to calculate empirical estimates of flood frequency (https://streamstats.usgs.gov/ss/) based on methods developed by Paretti et al. (2014). However, nearby stations with comparable characteristics in the bordering state of Nevada are not included. Thus, values are specifically tied to a watershed and characteristics can only be computed for Bronco Creek. Accordingly, the 0.2% annual exceedance probability (AEP) flood, that is, the 500-year flood, is 442 m^3/s for Bronco Creek, and the 1% AEP flood (the so-called 100-year flood) is 228 m^3/s.

The Eldorado Canyon study site is at the border between Arizona and Nevada, and its watershed can be reasonably considered to be within the same general region as Bronco Creek. We used the same method (Paretti et al., 2014), as applied by the USGS StreamStats service, for calculating the recurrence interval for Eldorado Canyon, because the sites are relatively close, though they are associated with contributing watersheds at different elevations. The 0.2% AEP (500-year) flood of Eldorado Canyon is calculated to be approximately 283 m^3/s.

2.2 | Characteristics of the two extreme floods

Both of our study sites experienced FMEEs that resulted from intense convective thunderstorms in summer months of the early 1970s. At Bronco Creek (Figure 1), a convective thunderstorm dropped approximately 76–89 mm of rain in less than 1 h on 19 August 1971, based on a rain gauge located ~3.2 km northwest of the basin centre (Aldridge, 1972). At Eldorado Canyon, a convective thunderstorm dropped 76–152 mm/h of precipitation during over approximately 1–1.5 h on 14 September 1974 (Glancy & Harmsen, 1975). Observers of this storm noted that it began near the headwaters and moved in a downstream direction, thereby increasing the amount of streamflow as it moved towards the mouth of the canyon. Rainfall totals from these events were approximately one third and half of the average annual rainfall (Table 1) of the nearest data sites: Wikieup, Arizona (Bronco Creek), and Searchlight (Eldorado Canyon), Nevada, respectively. According to the report by United States Department of Agriculture, Soil Conservation Service (1977), the Eldorado Canyon flood created a fresh fan delta in the lake that extended 91 m beyond the original shoreline at its junction with Lake Mohave. The flood also resulted in nine fatalities.

These extreme floods were FMEEs that obliterated vegetation in the channel system and extensively reworked the streambed braiding structure (Figure 3). Despite different studies and estimates, peak streamflows for each flood remain uncertain because of complex hydraulics and inadequate computational analyses at the time of the original post-flood measurements at each site. The original estimate for the Eldorado Canyon flood was 2152 m^3/s (Glancy & Harmsen, 1975), in the downstream part of the channel (Figure 3), that is, below the junction where the tributaries Eagle Wash and

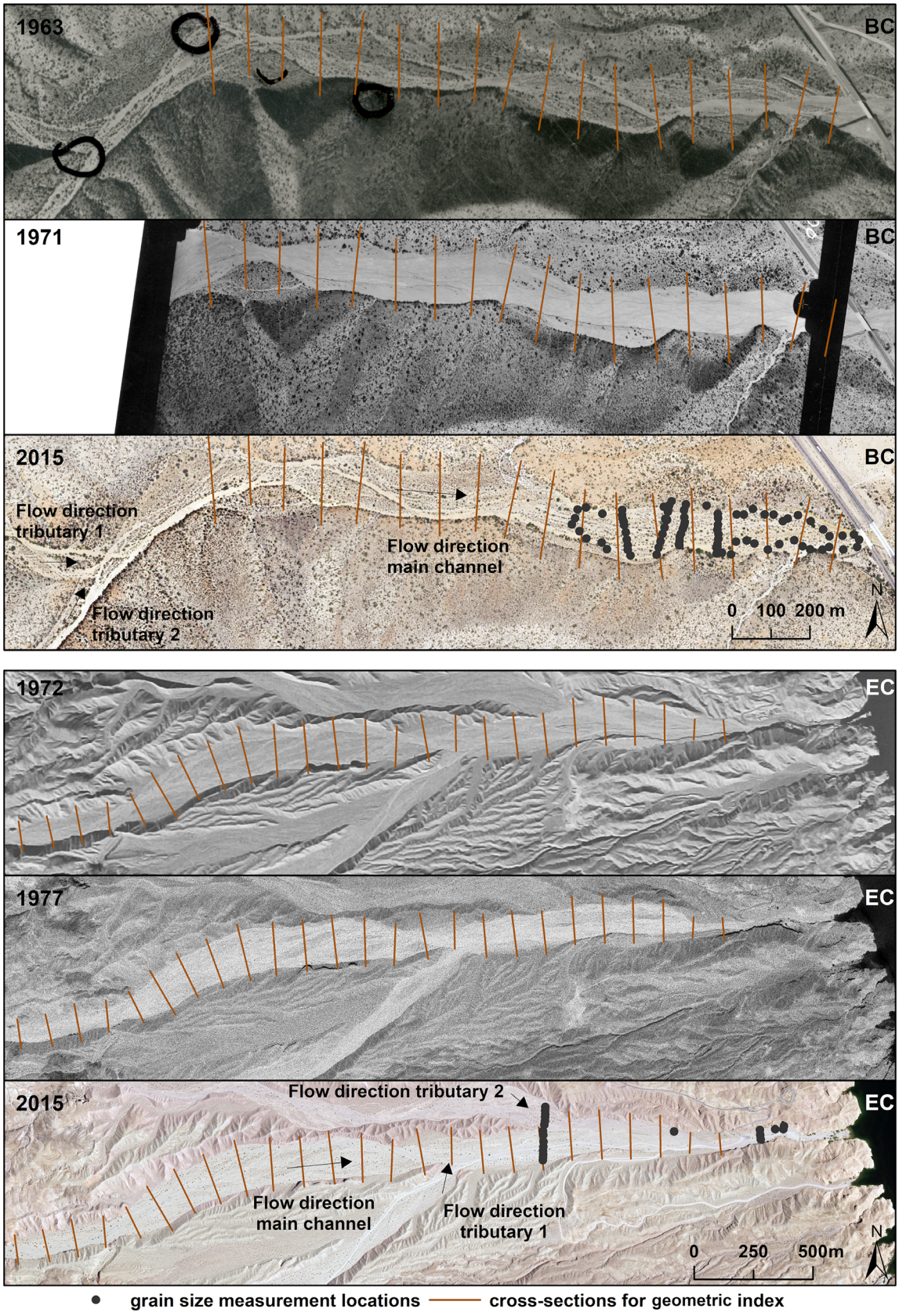

FIGURE 3 The pre-flood and post-flood aerial photographs of the study sites (EC, Eldorado Canyon flood in 1974, bottom 3 images; BC, Bronco Creek flood in 1971, top 3 images). The newest 2015 aerial photographs, which were used for the analyses, are also shown. The data sources are listed in Table 2. Bronco Creek 1971 aerial photographs cover less area than other photos in the series we analysed. The solid lines are the cross-sections where the flow line count (i.e., links of stream) was calculated, and the grain-size measurement locations are also shown as black dots (cf. Section 3). The black circles in the Bronco Creek 1963 aerial photograph are drawings of the ground control point locations measured during the field work in March 2013. At Bronco Creek, 'Tributary 1' is the outlet of both Bronco Creek and Greenwood Wash tributaries, which have their confluence further upstream, and 'Tributary 2' is Bronco Wash. At Eldorado Canyon, 'Tributary 2' is Techatticup Wash and 'Tributary 1' is Eagle Wash.

TABLE 2 Aerial photographs of Bronco Creek and Eldorado Canyon used in this study.

Bronco Creek: Time of aerial photograph	Producer/format (pixel size of digital data)	Eldorado Canyon: Time of aerial photograph	Producer/format (pixel size of digital data)
17.2.1954	USGS (2016a): Aerial photograph (1 m)	20.2.1954	USGS (2016a): Aerial photograph (1 m)
26.11.1963: Pre-flood	ADOT/AGS (scanned, 1200 dpi): Aerial photograph (0.00083 m)	20.1.1972: Pre-flood	USGS (2016a): Aerial photograph (0.00167 m)
20.9.1971: Post-flood	ADOT/AGS (scanned, 1200 dpi): Aerial photograph (0.00083 m)	3.6.1977: Post-flood	USGS (2016a): Aerial photograph (1 m)
6.6.1981	USGS (2016b): NHAP (0.00167 m)	4.10.1980	USGS (2016b): NHAP (1 m)
6.6.1990	ADOT/AGS (scanned, 1200 dpi): Aerial photograph (0.00083 m)	27.8.1992	USGS (2016e): DOQ GeoTIFF (1 m)
18.9.1995	ADOT/AGS (scanned, 1200 dpi): Aerial photograph (0.0008 m)	-	-
1.6.2005	USGS (2016c): Orthophoto (1 m)	1.6.2005	USGS (2016c): Orthophoto (1 m)
31.5.2015	USGS (2016d): GeoTIFF of NAIP (1 m)	28.5.2015	USGS (2016d): GeoTIFF of NAIP (1 m)

Note: The extreme flood occurred in 1971 at Bronco Creek and in 1974 at Eldorado Canyon. ADOT and AGS data were provided to us by the AZGS and the Nevada Bureau of Mines and Geology. USGS data have been downloaded from their EarthExplorer (cf. reference list for further details: USGS, 2016a, 2016b, 2016c, 2016d, 2016e). The original aerial photographs, which were scanned, did not inform the resolution; therefore, only the pixel size of the scanned images is provided.

Abbreviations: ADOT, Arizona Department of Transportation; AZGS, Arizona Geological Survey; DOQ, digital orthophoto quadrangle; dpi, dots per inch; NAIP, National Agriculture Imagery Program; NHAP, National High-Altitude Photography; USGS, US Geological Survey.

Techatticup Wash join the main channel. The estimated peak streamflows of 2081 m^3/s (Bronco Creek: Aldridge, 1972) and 2152 m^3/s (Eldorado Canyon: Glancy & Harmsen, 1975, Table 2) are at least 10 times the 500-year flood predicted by the method by Paretti et al. (2014) (cf. Section 2.1).

An early reassessment of the published streamflow estimate for the Bronco Creek flood was calculated as ~800 m^3/s by Carmody (1980) using average channel geometry and flow conditions reported by Aldridge (1972, 1978). House and Pearthree (1995) developed a similar estimate using techniques of paleoflood hydrology. However, due to eyewitness accounts of complex hydraulics ('roll waves'), untenable physical conditions implied by the original estimates and various ancillary data about the flood, a variety of estimates have been reported over the ensuing years. The newest estimate promulgated by the USGS (Costa & Jarrett, 2008) is that the peak streamflow was about 750–850 m^3/s (House & Pearthree, 1995), but that the total instantaneous streamflow associated with passing translatory wave crests was about 2740 m^3/s (Costa & Jarrett, 2008; Hjalmarson & Phillips, 1997; cf. House et al., 1998). Both streamflows exceed the 0.2% AEP (500-year recurrence interval) floods estimated in 'StreamStats' and using the regional regression equations of Paretti et al. (2014).

Despite lacking directly measured flow values and a gauging record, there is a solid body of direct and anecdotal evidence indicating that these two flood events were extreme (Glancy & Harmsen, 1975; House & Pearthree, 1995). Both are key historic floods known for their extremely large reported peak magnitudes in relation to drainage area. For example, Costa (1987) showed that they both accord with the (then) global envelope curve of drainage area versus peak streamflow. Also, Bullard (1986) assessed both events as analogues for the scales of floods that are of concern in dam safety analyses. Historically, those studies have relied on the concept of the probable maximum flood (PMF) based on rainfall–run-off models of extreme rainfall values. PMF is intended to be the worst-case scenario flood, and these two events approach values more than 50% of the computed/modelled PMFs for basins of that size (Bullard, 1986). Also, the revised estimate of the Bronco Creek peak streamflow as reported by House and Pearthree (1995) adheres to the trend of the regional maximum flood curve for the lower Colorado River Basin based on recorded data and paleoflood information (Enzel et al., 1993).

3 | DATA AND METHODS

3.1 | Aerial photographs and their processing

The dataset consists of aerial photographs of both Bronco Creek and Eldorado Canyon (Table 2). Decadal detection and comparison of the fluviomorphic trajectories are possible from 1954 to 2015. Similar decadal, or even sparser, datasets have been used in other ephemeral river studies and shown to be valid for detecting changes within the dryland environments of the region (Cadol et al., 2011). The photographs were selected based on their date and quality. In addition to freely downloadable aerial photographs from EarthExplorer of USGS (USGS, 2016a, 2016b, 2016c, 2016d, 2016e), we used hard-copy aerial photographs of Bronco Creek from the Arizona Department of Transportation (ADOT) and the Arizona Geological Survey (AZGS) (Table 2: cf. the photograph acquisition dates and details). These hard-copies were provided to us by the AZGS and the Nevada Bureau of Mines and Geology. These photographs were scanned with the maximum possible resolution (1200 dots per inch [dpi]). The pixel size of the scanned aerial photo was 0.00083 m. The pixel size was 0.00167–1 m in the case of other freely downloadable raw datasets (orthophotos, GeoTIFFs or data without coordinates).

The aerial photographs were georeferenced based on field surveys at Bronco Creek (by authors) in March 2013 and on orthorectified photos of years 2005 and 2015, which were downloaded from EarthExplorer (USGS, 2016a, 2016b, 2016c, 2016d, 2016e). During the field work, ground control points (GCPs) were measured with RTK-GPS (Figure 3). The GCP locations were selected from the objects that were visible in the hard-copy photographs from 1963 and 1995. The GCPs were located to span the entirety of the 1963 aerial photograph (note that only study reach part of this photograph is shown in Figure 3).

During georeferencing, the pixel size of each image was defined as 0.5 m to minimize possible quality reductions to the dataset and for not exceeding the 1-m resolution of some of the already georeferenced data (e.g., from 2005 to 2015 at the two study sites). The georeferencing was done in Eldorado Canyon using the nearest neighbour resampling method and spline transformation function based on GCPs (photos from years 1954, 1972, 1977 and 1980). In Bronco Creek, these methods were applied also to 1963, 1971 and 1995 photos. The orthorectification root-mean-square error (RMSE) values (forward in m and inverse in pixels) were basically zero in all these cases when spline was applied. However, the first-order polynomial transformation function and nearest neighbour resampling method resulted in the best orthorectification results for the years 1954 (total RMSE, forward: 5.427440 m; inverse: 3.757274 pixels), 1981 (total RMSE, forward: 4.911760 m; inverse: 0.001575 pixels) and 1990 (total RMSE, forward: 7.787527 m; inverse: 0.012093 pixels) of Bronco Creek. Data from other years were rectified by the data provider. Thus, during the georeferencing, we aimed for exact matches within the reach areas of interest (i.e., not in the edges of the images) between the data with pre-existing coordinates and the images to be rectified. The control points were always placed around the stream channel in question. All in all, the georectification error between the used control points was from near 0 up to 7.8 m in aerial photos. Overall, the matching within the study area was successful. The resolutions of each image (both georeferenced by author and by external free provider) are seen in Figures 4 and 5.

3.2 | The stream network analyses

We assume indices of stream connectivity that have been applied to identify occurrences of large streamflow events in perennial streams (e.g., Egozi & Ashmore, 2008) can also be used for ephemeral streams, as their stream-link structures represent geomorphic features developed while the channel is under streambed mobility conditions induced by competent water flow, though far more discontinuously as compared to perennial streams.

We analysed stream-link and bar areas on the orthorectified aerial photographs. In this paper, we use the term 'stream-link areas' to denote the non-vegetated channel thalweg areas where water was interpreted to have flowed during the lowest recent flood conditions relative to the age of the photos. Bar areas were defined as more stable features, often with at least some desert vegetation (Figures 4 and 5). The existence of desert vegetation is part of the stream-link area concept in our study. However, we did not perform specific analyses of vegetation interactions. We acknowledge that riparian vegetation can respond to and interact with changes in the channel morphology rather than driving channel change (Cadol et al., 2011).

All the photos in the series show no-flood conditions. The forms were created by the floods occurring between the photographs and closely resemble the planimetric braiding structures of perennial streams. Due to differences between the aerial image types, the characterization and delineation of the channel forms were done by manual mapping and digitization, as no automation was possible. Thus, the bar areas were digitized as distinct geomorphic elements and areas of bare sediment in between them (i.e., stream-link areas) were also mapped (Figures 4–6). We employed this dual classification to account for varying aerial image types that made consistent mapping of certain features difficult (e.g., bars of different relative ages). The areal coverages of the bar and stream-link areas of the channel were defined for each analysed time step, and the proportion (%) of the stream-link area relative to the total channel area was calculated. In addition, all the nodes of junctions (i.e., bifurcations and confluences) at the different ends of the bars (where stream-links join or separate) were digitized as points (Figure 6). Note that if the flow line division was not at the bar confluence or bifurcation location, no node was marked (cf. Figure 6). The point kernel density (n/m^2) within the 100-m radius of these nodes was calculated. Note that all junctions, both bifurcations and confluences, were combined in the density calculations. The development of the channel bar structure with time was evaluated based on these values defined from each aerial photograph in the series.

The geometric braiding index was calculated using the count of flow lines (or 'links') cut by the cross-section lines (Figures 3 and 6). This method has been used in other studies for a variety of braided riverbed structures. According to Egozi and Ashmore (2008), the channel count indices need a minimum of 10 cross-sections spaced no further apart than the average wetted width of the channel within the representative reach length. Thus, the cross-sections were defined in Eldorado Canyon at approximately every 150 m and in Bronco Creek at approximately every 90 m. Egozi and Ashmore (2008) describe three types of indices to characterize braiding stream-link and bar structures. We followed the approach of Chew and Ashmore (2001); that is, flow lines ('links') within the stream-link areas were counted along evenly spaced cross-sections. Then the index was calculated by averaging the values of all cross-sections at each analysed time step (called BI_{T3} type of index in the study of Egozi & Ashmore, 2008). This method (cf. Figure 6) was chosen because Egozi and Ashmore (2008) asserted that this type of channel count is most frequently used in correlating braided channel patterns with flow, stream power, sediment transport, morphology and vegetation parameters and also in observing variations over time under experimental conditions.

Pearson correlation was analysed between stream-link area (% of total area), maximum node density (n/m^2), mean node density (n/m^2) and geometric braiding index. Otherwise, the parameters were compared to each other, except the correlation between maximum and mean node densities was ignored, as those were based on the same original dataset. The analysis showed either a negative or positive correlation between parameters (cf. Section 4.5) with the possible range of values being from −1.0 to 1.0. The two-tailed t test was also included. The analyses showed whether the correlation was significant at the 0.05 or 0.01 level (p value).

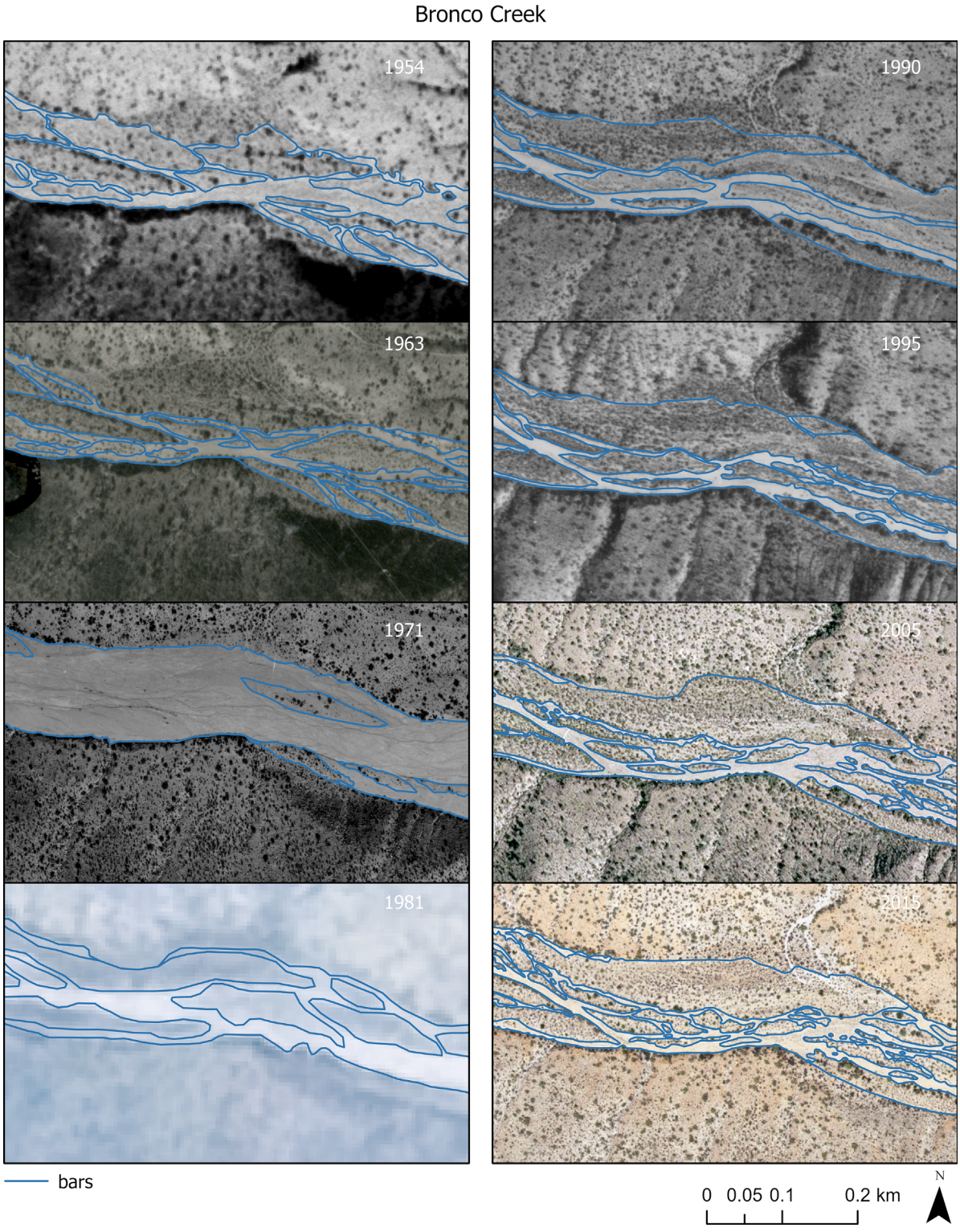

FIGURE 4 Close-up views of image resolution and mapping of bar and confluence nodes at Bronco Creek. Note that the 1981 image had the lowest resolution, but the dual classification between bar areas and stream-link areas was possible. Nodes were defined for bars that were clearly separate from each other, that is, had stream-link areas in between.

3.3 | The grain-size analyses

Grain sizes of the channel sediments were defined from Bronco Creek and Eldorado Canyon in March 2013 and January 2020, respectively (locations in Figure 3). In Bronco Creek, normal RGB camera photographs were taken throughout the downstream section of the channel. The locations (Figure 3) were selected cross-sectionally and along the banks, to cover the grain-size variation throughout the channel width (both bars and stream-link areas). The photos were taken approximately from ~1-m height (i.e., waist height of the photographer) and thus covered areas of ~0.5–1 m times 0.5 to 1-m land surface, depending on the photo, thus being slightly larger than 0.5 quadrats, for example, as used by Hooke (2007). A tape measure or scale was placed next to the gravel as

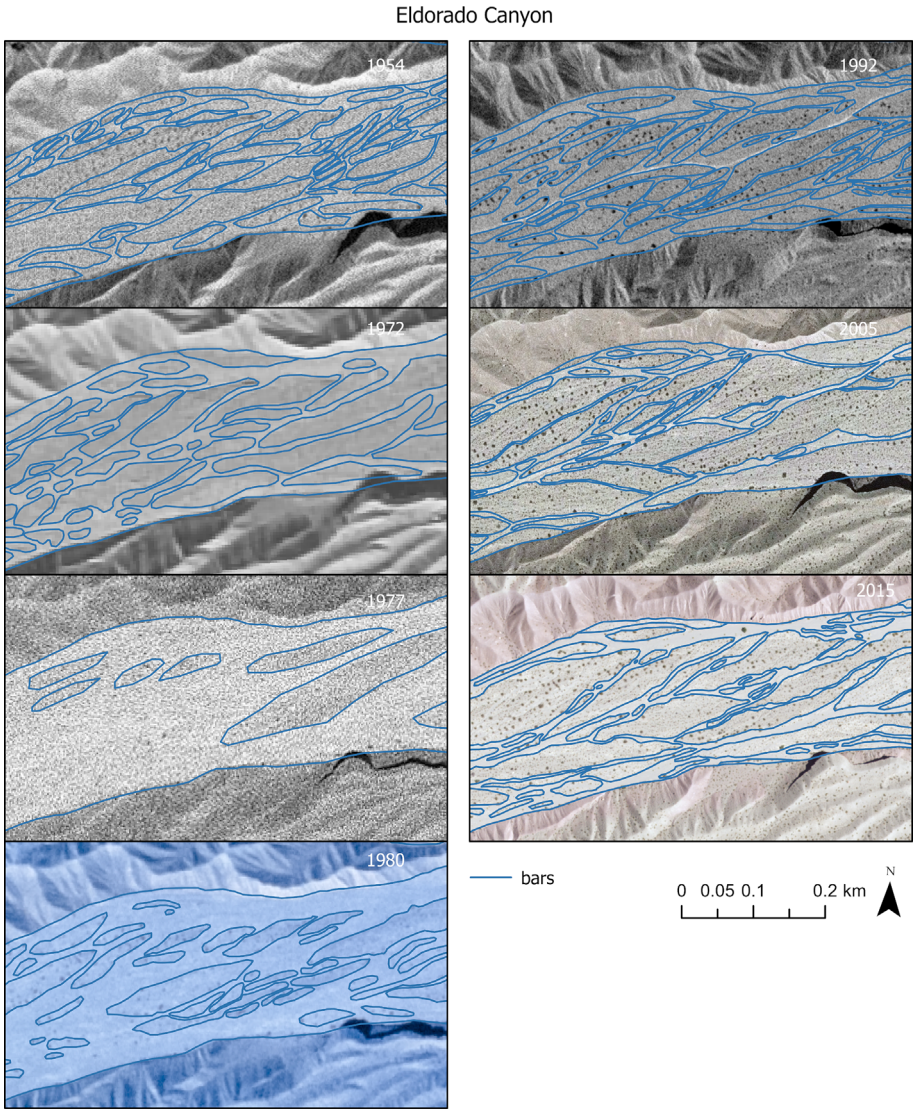

FIGURE 5 Close-up views of image resolution and how the bar and confluence node mapping looked at Eldorado Canyon. Note that the 1980 image had the lowest resolution, but the dual classification between bar areas and stream-link areas was possible. Nodes were defined for bars that were clearly separate from each other, that is, had stream-link areas in between.

shown in these photographs (Figure 7), and 67 locations were analysed in this way. The minimum grain size, as possible to detect from photographs, was 0.5 mm. Hooke (2007) had analysed the average grain sizes from each of their figures for enabling temporal detection from specific locations. In our study, the grain-size data were gathered to show the overall differences in the maximum grain sizes between the sites (i.e., the maximum particle size possible to entrain at peak flood discharge), not between specific locations. The largest visible clasts in each photo were chosen for calculating the (arithmetic and geometric) average maximum grain sizes of the studied reaches. The largest visible clast of each photo was selected based on manual measurements, and the *b*-axis maximum lengths of this clast were recorded from each photograph. Then the average maximum grain size was calculated for the whole study sites. For this analysis, manual detection was the most efficient method. In future work, systematic digital granulometric analysis could be employed for this type of data.

Similar grain-size analyses were made for two channel cross-sections in Eldorado Canyon based on photographs from January 2020 (Figures 3 and 7). The first cross-section was in the downstream part of Tributary 2 (seven photographs) and continued through the main channel (10 more photographs). The second was in the downstream part of the main channel (seven photographs). In addition, three photographs were taken from the main channel between those two cross-sections, and six photographs were taken downstream of the second cross-section. As in Bronco Creek, the maximum *b*-lengths were analysed from each photograph.

4 | RESULTS: THE EVOLUTION OF BRONCO CREEK AND ELDORADO CANYON SINCE 1954

4.1 | The grain sizes of Bronco Creek and Eldorado Canyon

The grain sizes of the study sites slightly differed from each other. In Bronco Creek, *b*-axis values ranged from 2.5 to 260 mm. These included granule, pebble, cobble and fine boulder classes according to the Udden–Wentworth scale (Wentworth, 1922). On average (arithmetic mean), the maximum grain size from the photograph measurements was 38.8 mm, which falls within the very coarse pebble class of the Udden–Wentworth classification. The geometric mean would be slightly less, that is, 27.1 mm. The maximum *b*-lengths varied from 80 to 430 mm in Tributary 2 of Eldorado Canyon, with the average (arithmetic mean) value being 195 mm. The maximum *b*-lengths of the

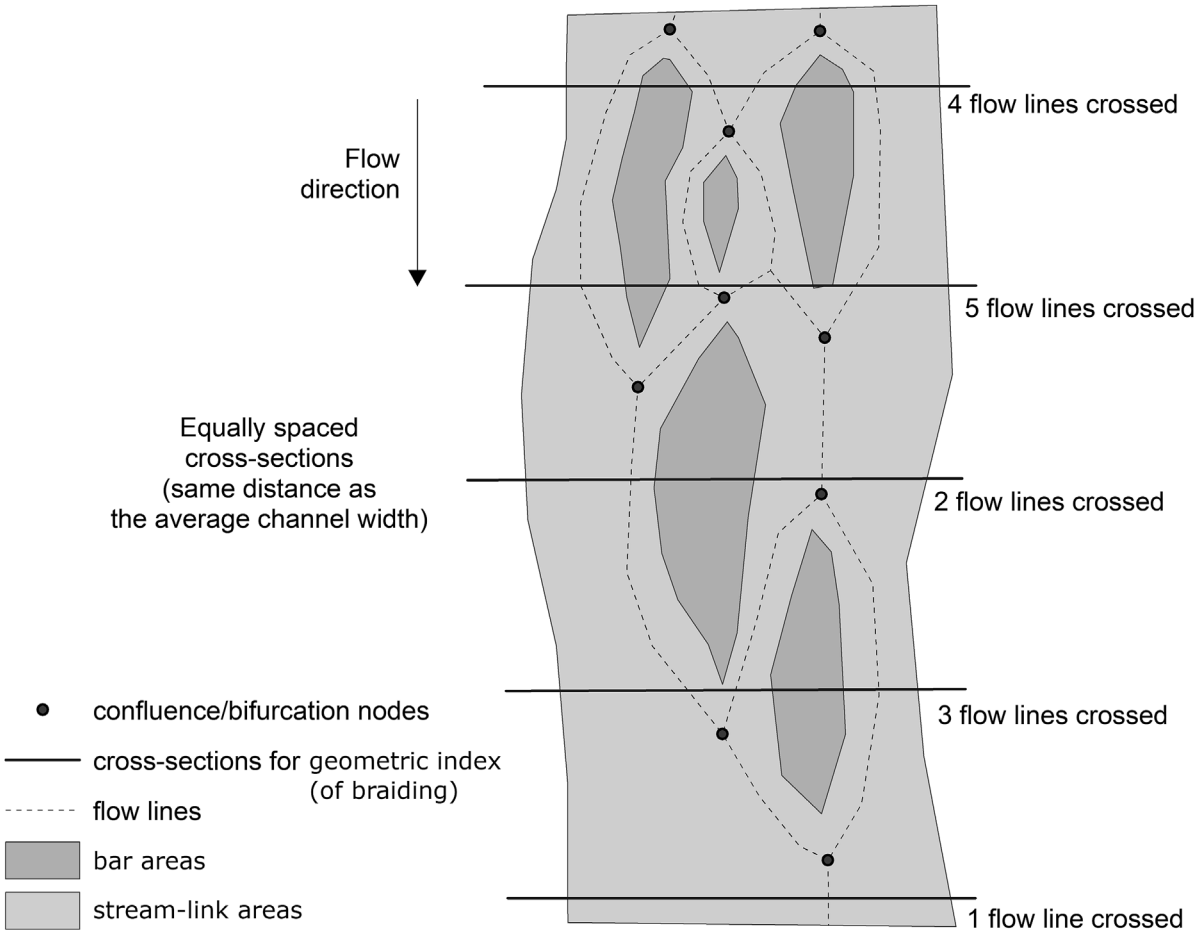

FIGURE 6 Schematic drawing of the geometric index calculation method for the braiding structures and division between stream-link and bar areas. The flow lines (or 'links') are in the middle of the stream-link areas, and their number is calculated per cross-section. Then their average count within the study site is defined for determining the geometric braiding index of each analysed time step. The junction, or confluence–bifurcation, nodes include the links at opposite ends of the bars as shown in the drawing.

main channel of Eldorado Canyon varied from 22 (pebble) to 370 mm (fine boulder), with the average (arithmetic mean) being 88 mm (cobble). When all these data were analysed together, the average (arithmetic mean) maximum *b*-lengths of Eldorado Canyon grain sizes were 110 mm. The geometric mean of these maximum *b*-lengths was 93.5 mm. Thus, the average maximum grain size (arithmetic and geometric) was approximately three times larger at Eldorado Canyon than at Bronco Creek, which is consistent with the steeper channel gradient at that site.

4.2 | The changes in stream-link areas since 1954

Our study results document key trends in ephemeral stream channel evolution following floods large enough to act as FMEEs. Based on visual interpretation, these two extreme floods obliterated pre-existing channel morphological features, removed almost all streambed vegetation and formed large, up-scaled bars in the streambed at each study site (Figure 3). For the Bronco Creek channel, the stream-link area increased from 34.9% to 86.5% of the total channel area after the FMEE of 1971 (Table 3 and Figure 8). In Eldorado Canyon, the proportion of stream-link area increased from 43.0% to 77.5% after the 1974 flood event. Thus, the FMEE resulted in a stream-link area increase of 51.6% for the Bronco Creek study site and 34.5% for the Eldorado Canyon site. The post-flood aerial photographs of Eldorado Canyon were from 1977, which resulted in a longer time gap between these post-flood aerial photographs and those used to document the flood in Bronco Creek, where the post-flood aerial photographs were taken less than a year after the event. This may partly explain the smaller stream-link area proportion in the post-flood photographs of Eldorado Canyon than in the ones of Bronco Creek. The precipitation data of nearby stations show that there have been rain events with potential for streamflow formation in the general study region during this period in both areas (Figure 2), but it is not certainly known the size or precise timing of the floods.

4.3 | The changes in junction-node densities since 1954

The densities of junction nodes were also substantially reduced by these extraordinary events. At Bronco Creek, the maximum junction-node densities did not approach the pre-flood values until about 25–35 years after the flooding (Figures 8 and 9). In addition, it took 30–35 years for the bar structures to become spatially distributed as uniformly as in the pre-flood situation (Figure 9). Note that this spatial distribution is based on a visual interpretation of the kernel density results. Even though the maximum node density was high in 1990,

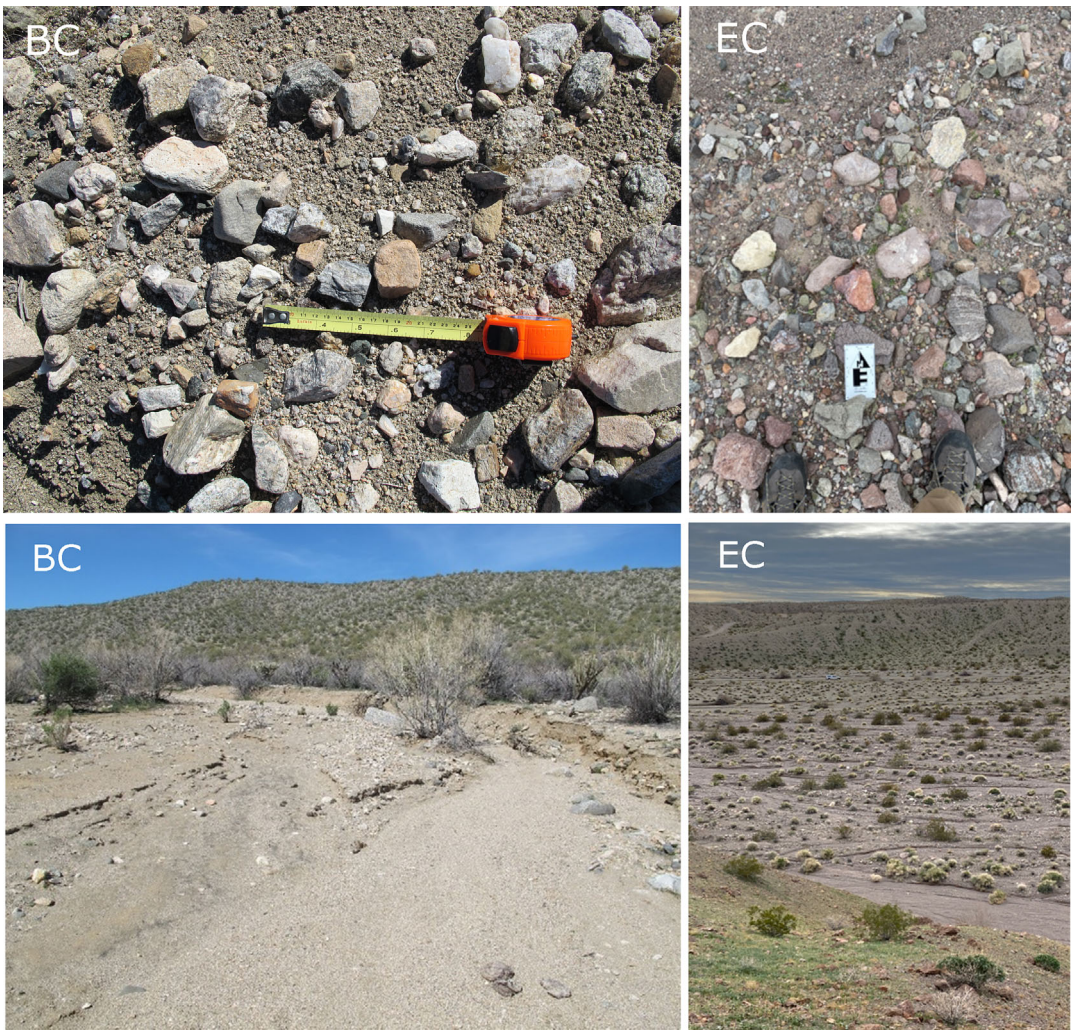

FIGURE 7 Selected terrestrial photographs (personal photos taken by the authors: BC in March 2013; EC in January 2020) showing the mainstem channel and representative grain sizes of the Bronco Creek and Eldorado Canyon study sites. The maximum grain size shown in the Eldorado Canyon photo is 12.2 cm, which is representative of the average maximum *b*-length grain size in the study reach. Note that the reference card in Eldorado Canyon measures 86 × 153 mm. Also, photos of the channels and their topography are shown at Bronco Creek and Eldorado Canyon. These show that the bar areas and stream-links are easily distinguished and the vegetation is sparse/scattered.

the nodes were not spatially distributed as uniformly as in 1963 or later in 2005. The highest density and most uniform spatial distribution of channel bars and their junction nodes were observed in the 2015 photographs. There had been larger bars in 1981 and 1990, and only after 1990 were the larger bars cut into smaller ones. Nevertheless, it is clear that floods with similar extraordinary impacts of fluviomorphic erasure have not occurred at the study site since the events of 1971.

At Eldorado Canyon, the maximum node densities were mostly larger than in Bronco Creek (Table 3 and Figure 8). For example, in 1954, the Eldorado Canyon study site had a junction-node density 2.4 times that of the Bronco Creek site, and in 2015, the comparative value was 1.4 times larger. This might be explained by the higher gradient and larger grain-size ranges for the Eldorado Canyon site, making the channel more prone to cutting and branch avulsion. Channel cut at Eldorado Canyon, that is, the bifurcation–confluence node density, increased between 2005 and 2015. But the spatial distribution of the node density was similar in the 1992 and 1954 data (Figure 10): There had been larger bars downstream of the two tributary junctions, and the upstream reach of the main channel had a higher node density during those years. Examination of aerial photographs from 2005 and 2015 reveals that the bifurcation–confluence node density had also increased in the downstream part of the study site. This indicates that before the aerial photographs of 1992, it is likely that there were streamflows capable of forming large bar structures in the downstream section. After 1992, the bars were also cut in the reach downstream of the tributary junctions. This is similar to Bronco Creek, where the node density reached in 2015 was the highest value of the whole study period.

4.4 | The stream-link area as indicator of fluviomorphic changes since 1954

When the rates of the processes are calculated (Table 4), it is evident that the stream-link area decreased the fastest in the decade following the extraordinary flood event, that is, about 3.6% per year during the 1971–1981 period for Bronco Creek and about 4.1% per

TABLE 3 The evolution of stream-link area and node density at Bronco Creek and Eldorado Canyon, 1954–2015.

	Total area (m^2)	Stream-link area (m^2)	Stream-link area, % of total area	Max node density (n/m^2)	Mean node density (n/m^2)	Standard deviation of node density (n/m^2)	Geometric braiding index (BI_{T3} of Egozi & Ashmore, 2008)
Bronco Creek							
1954	240 889	86 886	36.07	0.00077	0.00024	0.00014	3.67
1963: Pre-flood	231 903	80 873	34.87	0.00069	0.00028	0.00014	3.83
1971: Post-flood	198 948	172 084	86.50	0.00049	0.00008	0.00009	1.61
1981	254 780	127 824	50.24	0.00036	0.00012	0.00008	2.89
1990	254 430	76 592	30.10	0.00090	0.00019	0.00017	3.39
1995	277 945	74 110	26.66	0.00085	0.00025	0.00019	3.67
2005	251 269	71 667	28.52	0.00080	0.00030	0.00018	4.28
2015	274 227	79 766	29.09	0.00141	0.00060	0.00028	5.39
Eldorado Canyon							
1954	618 392	153 351	24.80	0.00185	0.00035	0.00032	5.2
1972: Pre-flood	634 900	273 115	43.02	0.00109	0.00034	0.00021	5.2
1977: Post-flood	622 973	483 038	77.54	0.00034	0.00005	0.00007	1.64
1980	622 344	406 631	65.34	0.00084	0.00027	0.00019	3.48
1992	623 185	180 809	29.01	0.00153	0.00045	0.00029	6.52
2005	627 809	135 248	21.54	0.00194	0.00050	0.00037	5.68
2015	627 206	225 809	36.00	0.00200	0.00056	0.00032	6.6

Note: See also graphical presentation of these results from Figure 8. Note that the 1971 post-flood photographs of Bronco Creek covered a smaller area than in other years. The density values are calculated from the density analysis areas presented in Figures 9 and 10. The geometric braiding index was based on count of flow lines, that is, links (cf. Figure 3). There were 18 cross-sections in Bronco Creek and 25 cross-sections in Eldorado Canyon within the area covered by available aerial photographs. The flow line ('link') count of these cross-sections was the basis of the geometric index calculation.

year during the 1977–1980 (3-year) period for Eldorado Canyon. Also, the period 1980–1992 (12 years) of Eldorado Canyon saw about a 3% decrease per year in the stream-link area. The reduction in stream-link area decreased gradually in both streams after this period of about 10 years. Moreover, there was again a gradual increase in the stream-link area in Bronco Creek after 1995 and in Eldorado Canyon after 2005. These changes occurred because of the dissection of the bars, which increased the nodal density (Table 4). It can be assumed that the streamflow events capable of cutting the larger bars occurred between the 2005 and 2015 aerial images in both channels, as the node density of both bifurcations and confluences also increased throughout each study area (Figures 8–10).

Overall, the recovery time, that is, the time for the streams to reach their pre-flood values of the bifurcation–confluence densities, and stream-link area's proportion of the channel were similar for both Eldorado Canyon and Bronco Creek (Table 3 and Figures 9 and 10). At both sites, the bifurcation–confluence node densities increased first around and downstream of the narrow channel sections. Higher densities for the bifurcation–confluence nodes occurred also at the tributary junctions. Thus, channel evolution did not occur uniformly through the system during the first decades following the extreme flood. The proportion of stream-link area reached the pre-flood value within approximately 20 years at Bronco Creek (Table 3). In Eldorado Canyon, both the overall proportion of stream-link area and node density had reached the 1954 pre-flood values between 1992 and 2005. In other words, the stream-link area and maximum node density reached the pre-flood values within about 25 years.

4.5 | The changes in geometric index of braiding since 1954

The extreme floods of the 1970s resulted in decreased values of the geometric index of braiding at Bronco Creek (−56%) and Eldorado Canyon (−68%), which were 1.61 and 1.64 post-flood and 3.67 and 5.2 pre-flood (1954), respectively (Table 3). In Bronco Creek, the index for 1995 (i.e., 24 years after the extreme flood) was the same as in 1954. In Eldorado Canyon, the pre-flood geometric index value was regained sometime between 1980 and 1992, but closer to the end of the 1980s. Thus, in Eldorado Canyon, the recovery time of the index value was only about 15 years. Note that the index value of Eldorado Canyon was less in 2005 than in 1992. This differs from Bronco Creek, where the geometric index value consistently increased from year to year. In Eldorado Canyon, the situation became more static or had similarly high values in both periods 1992–2015 and 1954–1972. This indicates that the channel recovered more quickly than in Bronco Creek. This could be due to the differences in the gradient and grain sizes between the two study sites or because of different histories of low-to-moderate flood events. However, there are no proximal rain gauge data from the full observation period of Eldorado Canyon to validate the flood event history. The rainfall data from Wikieup, 3.7 km from Bronco Creek, indicates that there have been moderate rain events each year (cf. Figure 2 and study site section).

When all the parameter values were compared with each other, the Pearson correlation showed that, at Bronco Creek, there was a

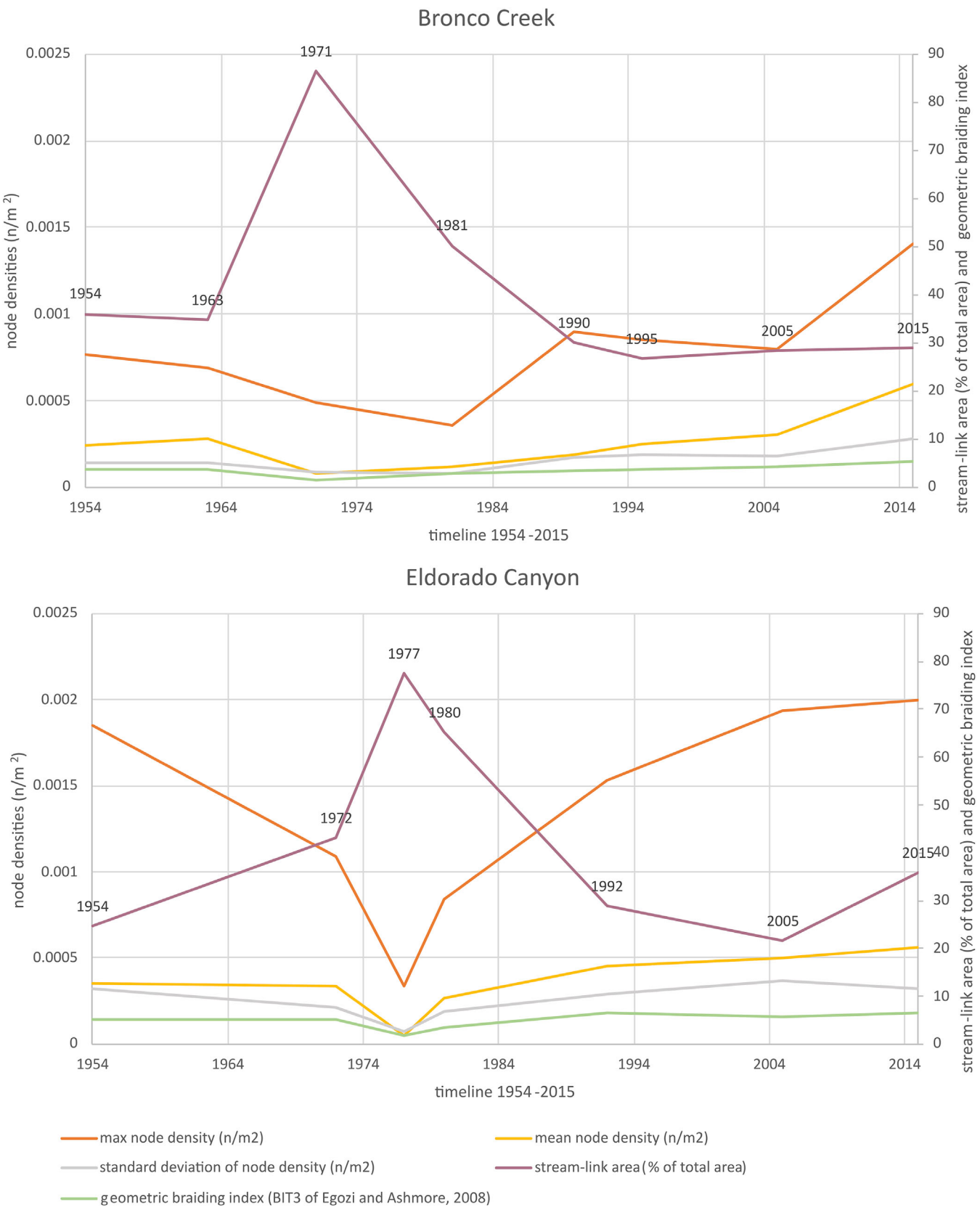

FIGURE 8 The evolution of stream-link area (% of total area), node densities (n/m^2), and braiding index at Bronco Creek and Eldorado Canyon, 1954–2015. See also the numerical presentation of these results in Table 3. The years of used data are presented as labels above the line showing the stream-link area. Eldorado Canyon (1977) and Bronco Creek (1971) year data depict the post-flood conditions.

positive correlation between geometric braiding index and maximum node density (0.831, significant at the 0.05 level) and mean node density (0.925, significant at the 0.01 level). Also, a significant (at the 0.05 level) negative correlation was found between geometric braiding index and stream-link area (−0.834). However, a non-significant correlation was found between maximum node density and stream-link area (−0.602) and between mean node density and stream-link area (−0.591). At Eldorado Canyon, similarly, geometric braiding index was

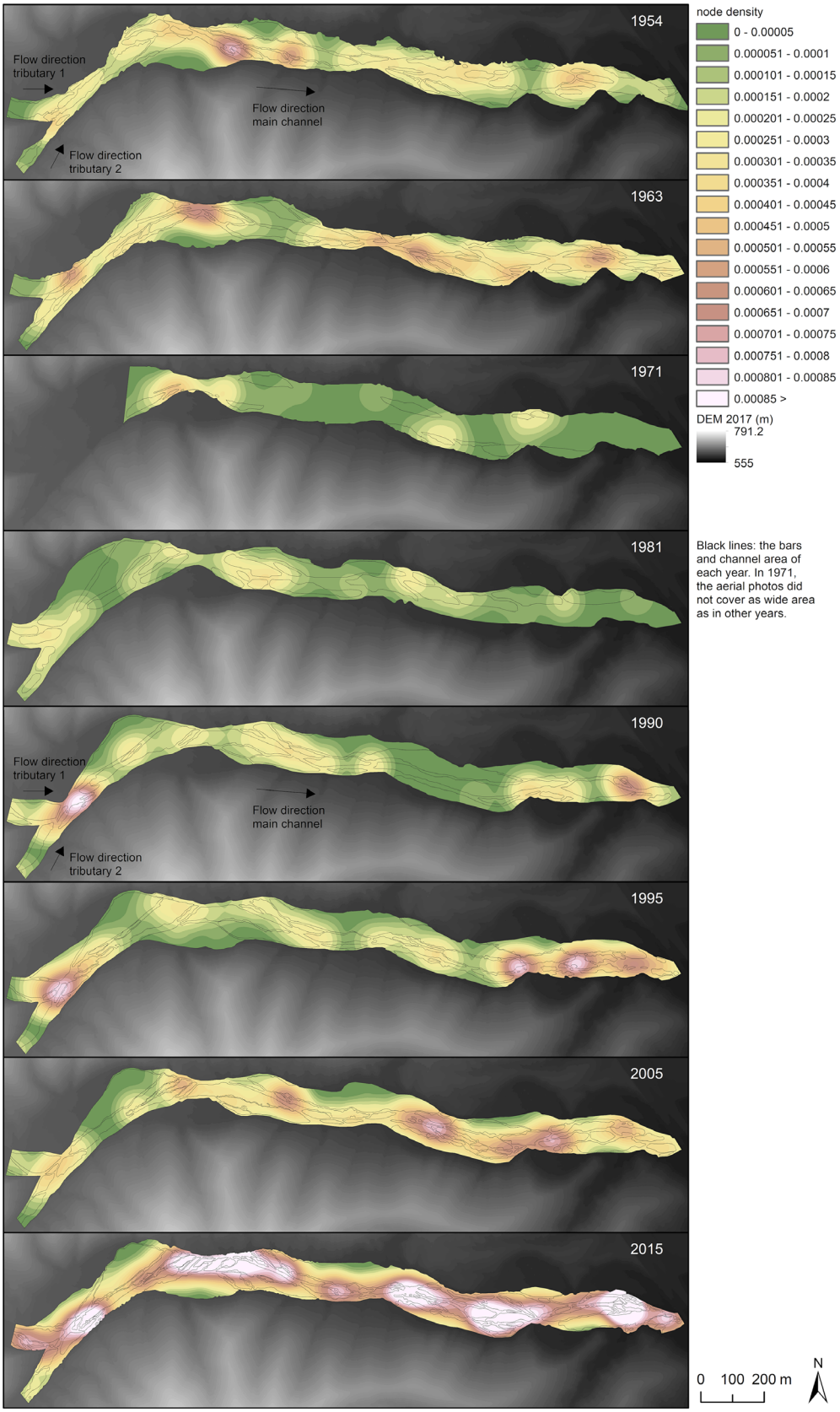

FIGURE 9 The spatial distribution of bedforms and bifurcation–confluence node densities (n/m^2, kernel density method) from 1954, 1963, 1971, 1981, 1990, 1995, 2005 and 2015 at Bronco Creek. The major flood occurred on 19 August 1971. The data of 1971 are from after the flood. Note the progressively more uniform distribution of nodal density foci over time since the (19 August) 1971 flood. An apparent interruption in the development of the pattern in the 1981–1990/1995 time frame likely reflects the occurrence of a relatively large flood that went otherwise unrecorded. The elevation model (1-m cell size), which is presented around the channel area, has been created from the photogrammetrically produced point cloud of 2017 National Agriculture Imagery Program (NAIP) data by the University of Arizona. These datasets are freely downloadable from the university libraries of the University of Arizona (source: http://libguides.library.arizona.edu/GIS/ImageryandLidar#), and the primary source is at https://catalog.data.gov/dataset/national-agriculture-imagery-program-naip.

correlated with maximum node density (0.882, significant at the 0.01 level), mean node density (0.954, significant at the 0.01 level) and stream-link area (−0.885, significant at the 0.01 level). However, correlation was also significant between mean node density and stream-link area (−0.839, significant at the 0.05 level) and between maximum node density and stream-link area (−0.928, significant at the 0.01 level).

In summary, it took approximately 25 years for both the Eldorado Canyon and Bronco Creek study sites to reach their pre-flood values for all three parameters: nodal density, stream-link area percentage and geometric braiding index. After that time, streamflows of unknown magnitude further dissected large bars into smaller ones at both sites. There have been moderate rainfall events throughout the

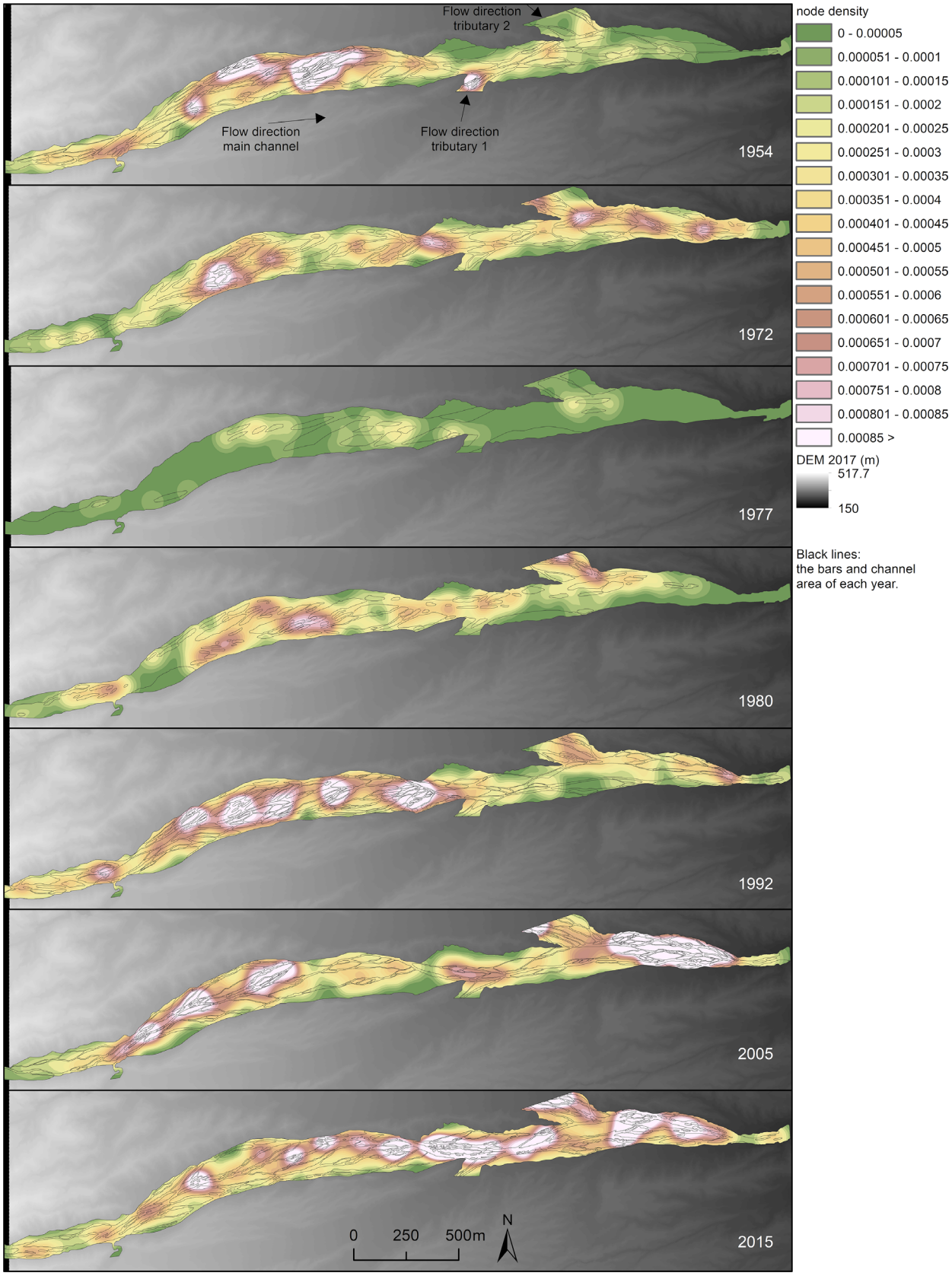

FIGURE 10 The spatial distribution of bedforms and bifurcation–confluence node densities (n/m^2, kernel density method) since 1954 at Eldorado Canyon. The flood occurred on 14 September 1974. The elevation model (1-m cell size), which is presented around the channel area, has been created from the photogrammetrically produced point cloud of 2017 National Agriculture Imagery Program (NAIP) data by the University of Arizona. These datasets are freely downloadable from the university libraries of the University of Arizona (source: http://libguides.library.arizona.edu/GIS/ImageryandLidar#), and the primary source is at https://catalog.data.gov/dataset/national-agriculture-imagery-program-naip. Note the progressively more uniform distribution of the nodal density foci over time since the flood.

TABLE 4 The changes in maximum node density and percentage of stream-link area per year within the detected time periods.

Year	Time period length, years since previous aerial photograph	Stream-link area % of total channel area, change within time period	Max node density (n/m^2), change within time period	Stream-link area % of total channel area, change per year within time period	Max node density (n/m^2), change per year within time period
BC					
1954	-				
1963: Pre-flood	9	−1.20	−0.000080	−0.13	−0.000009
1971: Post-flood	8	51.63	−0.000200	6.45	−0.000025
1981	10	−36.26	−0.000130	−3.63	−0.000013
1990	9	−20.14	0.000540	−2.24	0.000060
1995	5	−3.44	−0.000050	−0.69	−0.000010
2005	10	1.86	−0.000050	0.19	−0.000005
2015	10	0.57	0.000610	0.06	0.000061
EC					
1954	-				
1972: Pre-flood	18	18.22	−0.000760	1.01	−0.000042
1977: Post-flood	5	34.52	−0.000750	6.90	−0.000150
1980	3	−12.20	0.000500	−4.07	0.000167
1992	12	−36.33	0.000690	−3.03	0.000058
2005	13	−7.47	0.000410	−0.57	0.000032
2015	10	14.46	0.000060	1.45	0.000006

Abbreviations: BC, Bronco Creek; EC, Eldorado Canyon.

existing data record periods, but the data are non-existent from the most recent years of Searchlight station, which would have been the closest to Eldorado Canyon. It is also unknown how many of these rainfall events produced streamflows in these channels, despite the thresholds for potential streamflow in the greater region having been exceeded each year (Figure 2).

5 | DISCUSSION

5.1 | The fluviomorphic trajectories of Bronco Creek and Eldorado Canyon

Our study results document key trends in ephemeral stream channel evolution following FMEEs, and our study sites are representative of drainages throughout large parts of the US desert southwest and other deserts around the globe. The results advance general understanding of rates of dryland stream channel evolution and recovery from FMEE-type floods that are likely to become larger and more frequent in the coming decades, particularly due to the climate-related increases in precipitation intensities and amounts that are anticipated for the southwestern United States (Hawkins et al., 2015; IPCC, 2021; Pascale et al., 2019; Tousi et al., 2021).

The future climate change relevant to applications of our study results is on the decadal scales that are most influenced by human-induced factors (IPCC, 2021), though an interesting possibility is that increasing sea-surface temperatures in the Gulf of California might indirectly increase alluvial fan aggradation (Miller et al., 2010). This could then impact some ephemeral channel systems. In the past, at least, there have been important multi-centennial fluctuations in flood frequencies and magnitudes in the southwestern United States (Bacon et al., 2010; Miller et al., 2010), which have generally been correlated to various natural ancient climate events and long-term trends.

Despite uncertainties about expected future changes, our study results remain applicable to recovery times, given the multi-decadal scale and temporal resolution of our data series. Our study highlights the value of using historical aerial photo data to detect the occurrence and approximate timing of past extraordinary flood occurrences in ephemeral dryland streams. We have shown that extremely large floods can leave obvious visual evidence of their occurrence, and that their primary effect is a simplification of the drainage pattern and the channel bed morphology. Similar to results for an ephemeral stream in Spain (Sanchis-Ibor et al., 2015), the large floods at Bronco Creek and Eldorado Canyon resulted in decreased geometric (braiding) index values. It took a couple of decades before the subsequently appearing larger bars were cut into smaller ones. This indicated the occurrence of streamflow events capable of dissecting large bar structures (Lotsari et al., 2018), showing that the effects of the extraordinarily large floods were slowly ameliorated by more frequent floods of lower magnitude. Moreover, the cumulative impact of the small floods on bed morphology occurred over many years during which there was a general lack of flood events large enough to disrupt the developing pattern. This amelioration occurred mostly through fluvial processes with varying degrees of interaction with desert riparian plants, the slow growth of which likely contributed to channel bar stabilization.

Vegetation for our study sites differs markedly from the riparian woodlands of dryland streams for which a rather high streamflow threshold needs to be overcome to generate channel widening (Friedman & Lee, 2002). For Bronco Creek and Eldorado Canyon,

based on our results, any threshold effect of the desert vegetation only impacts the channel bars, becoming insignificant in the case of the most extreme floods. We note that the existence of desert vegetation is part of the stream-link area concept in this present study and acknowledge that vegetation growth could be important in the recovery process. Our study was able to document the channel morphological impacts of lower magnitude fluvial processes, using indices of channel network complexity to characterize the time-dependent effects of low-to-moderate floods (e.g., stream-link connectivity/node density assessments). A stronger focus on vegetation effects could likely enhance future studies.

It took approximately 25 years for our study sites to reach their pre-flood values of all three parameters: nodal density, stream-link area percentage and geometric braiding index. After the FMEEs in the early 1970s, streamflows of unknown, but much lower magnitudes occurred, and dissection of large bars into smaller ones occurred at both study sites. Based on previous literature, these subsequent floods would need to have been moderate within the context of the reach to dissect the relict and larger bar structures (Lotsari et al., 2018). Precipitation data from nearby observation stations reveal occasional precipitation events that exceeded thresholds (i.e., 3–13 mm: Kampf et al., 2018) for potential streamflow generation, but there are no direct data on how many of the precipitation events resulted in flood events.

The spatial distribution of each of the measured parameters took the longest to revert to pre-flood conditions. Around 30–35 years after the FMEEs, bar formation became more widely and uniformly spread throughout the study areas, and the spatial distribution of the bifurcation–confluence nodal density reached the pre-flood condition. Concurrently, the stream-link area started to gradually increase. If streamflow events occurred more frequently in the late 1990s, and especially between 2005 and 2015, this would explain the increase in the number of bar confluences and bifurcations, and stream-link area, as well as the more uniform spatial distribution of the nodes on both streams after 30–35 years. The bar formation that became more widely and evenly spread throughout the study areas could have resulted from interacting streamflow events with the co-evolution of vegetation growth, as was observed in the study by Cadol et al. (2011). If extreme floods were to become more frequent in the future, as climate models suggest, the channel recovery process that we have measured could be disrupted and erased at an increased frequency, thus promoting a quasi-equilibrium of the geomorphic trajectory of the stream systems and their attendant desert riparian plant communities.

Our study shows that the channel amelioration process (1) is easily documented in this environment, (2) is time dependent and (3) is reset periodically by large to extreme floods. Generalizing these results, Figure 11 shows how a hypothetical flood series for dryland ephemeral streams correlates with concurrent changes in channel pattern complexity. The transformation and subsequent amelioration of the channel can be a markedly discontinuous process because of a highly variable flood series including a mix of low floods, no-flood years and large to extraordinary floods.

The results of our temporal analyses of channel network evolution and recovery suggest that a duration of 30–35 years could represent either (1) the time required for the flow network to reach a quasi-equilibrium state or (2) a temporal spacing of floods large enough to have an adequate erasure effect on the channel morphology (Figure 11). Support for the latter interpretation is provided at Eldorado Canyon, where a large flash flood occurred on September 12, 1939 (United States Department of Agriculture, Soil Conservation

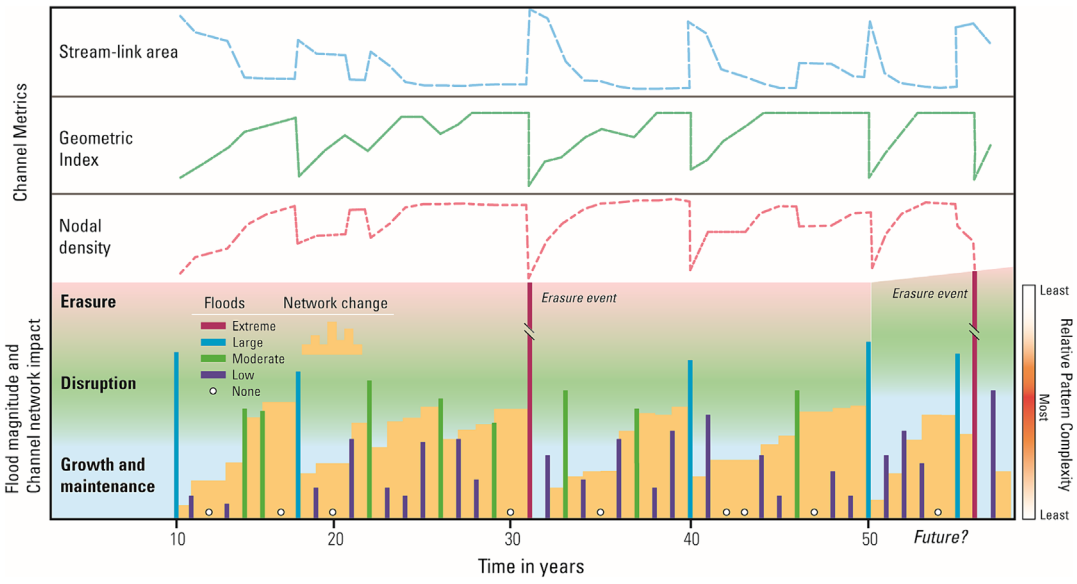

FIGURE 11 Schematic diagram of a hypothetical flood series for a steep dryland alluvial and ephemeral stream and concurrent changes in channel pattern complexity. The upper part of the diagram shows generalized and schematic trends in the measures of channel network geometry and complexity explored in this study. The flood series in the lower part of the diagram is shown over fields of colour that represent three distinct phases of channel network maintenance, disruption (minor to moderate change) and erasure (near complete to complete erasure of a complex network following an extreme flood). Gradations between these categories are diffuse. The tallest flood bar is the analogue for the fluviomorphic erasure events (FMEEs) investigated in this paper. The first tall flood bar is the proposed analogue for the FMEEs of the 1970s, and the second one in the series is somewhat taller for the purposes of speculating the influence of greater precipitation intensities that could result from a warming climate. This diagram was inspired by fig. 8 in Kochel (1988).

Service, 1977). The 1939 flood was centred in the Eldorado Canyon area and between Boulder City, NV, and Kingman, AZ. Notably, this event resulted from an El Niño-enhanced tropical storm incursion into the region that was part of a series of four tropical disturbances in September 1939 (Gatewood et al., 1946). According to Ziaco et al. (2020), increased precipitation occurred in the 1980s and early 1990s relative to previous or following years/decades along the southern escarpment of the Colorado Plateau on the Arizona–New Mexico border. This coincides with the timing (between 1980s and 1990s photos) when the density of bifurcations and confluences started to appear at both study sites. The long-term precipitation dataset, especially from Wikieup (close to Bronco Creek), shows that more frequent rain events occurred in the 1980s than during the latter portions of the 1990s or 2000s (cf. study site). As there are no data available since 1991 from a station near Eldorado Canyon, the time periods cannot be compared for that region.

Stream-link area decreased the fastest in the decade following the FMEEs, that is, about 3.6% per year during the 1971–1981 period for Bronco Creek and about 4.1% per year during the 1977–1980 (3-year) period for Eldorado Canyon. Also, the period 1980–1992 at Eldorado Canyon had about a 3% decrease per year in the stream-link area. The reduction in stream-link area decreased gradually for both streams after this period of about 10 years. The shape of the development of the analysed parameters at Bronco Creek and Eldorado Canyon has some similarities to a rate law function (Graph D in fig. 2 of Graf, 1977, following Knox, 1972). The initially rapid changes in stream-link area observed at Bronco Creek and Eldorado Canyon, followed by a gradual and discontinuous reduction in stream-link area, are generally consistent with Graf's (1977) basic concept. Whereas Graf (1977) used as the decay metric changes in length over time for three very small gullies near Denver, Colorado, our study tracks changes in the proportion of channel area and the degree of channel connectivity in a reach of constant length in a system that shows a tendency towards braiding over time. Because our focus is on rare and instantaneous FMEEs in desert streams, it is inevitable that the amelioration process occurs more slowly, but the rate at which it may progressively slow or 'relax' is difficult to determine from our dataset. Furthermore, it is likely that the erasure and subsequent recovery of the channel are discontinuous due to the relative rarity of moderate-to-high flood events (Figure 11). In general, the geometric characteristics are proxies for the relative complexity of the patterns wherein the pattern following an FMEE is the simplest, and the recovery over a post-erasure period of ~15–25 years results in a net increase in complexity. The flood series presented in Figure 11 is highly variable and includes events ranging from no-flow to large and extraordinary floods. The FMEEs in Bronco Creek and Eldorado Canyon were greater than 500-year floods in their magnitude, according to empirical models.

Discontinuous processes and the inherent role of temporal ordering of geomorphic events are important themes for interpreting and conceptualizing the post-flood recovery of rivers and streams in arid settings (Kochel, 1988; Wolman & Gerson, 1978). Kochel (1988) represented this concept by showing (his fig. 8) that recovery from a catastrophic flood in a fluvial system will follow a trajectory governed by smaller and more frequent events. His conceptual model also predicts that, early in the trajectory, the system will be less sensitive to the effects of moderate-to-large flood events because a catastrophic flood will have determined the relevant morphology. As the system continues to evolve, however, it will follow a steady path of adjusting to dominance by lower magnitude floods, while also increasing in sensitivity to disruption by another catastrophic flood. The latter can then terminate this sequence and initiate a new one. Kochel's model assumes a relatively long spacing between catastrophic flood events, but it also provides a framework for considering how variance can occur in the relation between progressively increasing sensitivity to flood-wrought geomorphic change and how the frequency of floods can impart catastrophic change. Our model (Figure 11) differs slightly from Kochel's because the 'recovery' variables that we measured develop more quickly than in the system that he envisioned. But the core concept remains: that arid region fluvial systems are likely to approach a quasi-steady state of channel morphology dominated by typically low-to-medium floods on decadal time scales, only to be completely interrupted by a singular catastrophic event that starts the process sequence all over again. Where the system might happen to lie on its fluviomorphic evolutionary trajectory will influence just how severe the catastrophic response will be.

5.2 | The uncertainties and prospects related to the analyses of fluviomorphic trajectories

Because both study area datasets were comparable in temporal detail, it was possible to develop an approximate measure of the pace of amelioration for their ephemeral channels. The only relatively long gap occurs for Eldorado Canyon, where high-quality aerial photographs were not found for the interval 1954–1972. More photographs could also have helped document a period in the late 1980s when bifurcations and confluences started to appear more spatially dense at both study sites. Nevertheless, our study has more detailed time-series documentation than other studies done in Arizona. For example, Cadol et al. (2011) applied six aerial photos to document channel narrowing in Canyon de Chelly, a much larger ephemeral drainage system in a different physiographic region from our study sites. Graf (1981) defined stable and unstable meander sections of a very large central Arizona river using approximately decadal historical map and aerial photograph data from 1868 to 1980, but unlike our study sites, the river channel had stable sections controlled by bed-rock or man-made structures.

Due to the lack of measured streamflow data, it was impossible to compare differences in the extreme flood hydrographs and hydraulics for both the Eldorado Canyon and Bronco Creek. Related data for the Big Sandy River and Lake Mohave, to which Bronco Creek and Eldorado Canyon drain, respectively, indicate the main river and reservoir (lake) stage changes coincident with the Bronco Creek and Eldorado Canyon floods. Though there are many caveats in correlating these stage changes to the Bronco and Eldorado flood magnitudes, it can be reasonably hypothesized, also invoking results from the Rambla de la Viuda in Spain (Calle et al., 2015; Lotsari et al., 2018), that the flood recession phases were capable of impacting fluviomorphic changes. In addition, volumetric change analyses were not possible due to a lack of time series of topographical data. Thus, we cannot compare our results to those from studies such as that of Ortega et al. (2014) regarding sediment delivery by flash floods. According to Hooke (2007), different events, even of the same size at the same site, can have differing impacts on ephemeral river channels,

and therefore, long periods of monitoring topography, vegetation and sediment would be necessary to analyse complex behaviour and linkages among these parameters. Hooke (2016a) states that the resistance of the channel to erosion relates to the bed material and its size. Thus, Bronco Creek and Eldorado Canyon could be more resistant to floods, due to their coarser grain sizes, than the channels of some previous studies, such as by Hooke (2016a). Longer term data series, also with higher temporal resolution, would be needed for detailed analyses of such interacting parameters.

The results of the present study could prove useful for comparisons to 'natural state' ephemeral channels in other regions, as well as to those influenced by major human action, such as gravel mining. Recovery time periods for such ephemeral streams, that is, where gravel mining has been the initial extraordinary event clearing the channel, have included increases in dense vegetation and decreases in sinuosity, and these streams have adopted a wandering pattern (Calle et al., 2015; Sanchis-Ibor et al., 2015). Further detailed analyses of the recovery times are needed in different types of natural and modified ephemeral channels of dryland environments. Knowledge of recovery trajectories will be especially important for restoration purposes in the ephemeral channels (Sanchis-Ibor et al., 2015). The present study shows the application potential of this method, so we agree with Sanchis-Ibor et al. (2015) and with the conclusion of Brierley and Fryirs (2016) that fluviomorphic trajectories, in addition to showing how the past has shaped the present, can also identify evolutionary trends for the management of river futures.

6 | CONCLUSIONS

Based on the results of this study, we conclude the following about the evolution of these two near-pristine ephemeral and alluvial stream channels in the southwestern United States. Extraordinary floods in dryland ephemeral alluvial streams (having a slope of 1.5–3.2°) generate vegetation-free channels with a small number of relatively large bar structures, increase the extent of stream-link area, reduce the density of bifurcation–confluence nodes and reduce the magnitude of the overall geometric index of braiding of the channel system. Maximization of these effects results in geomorphic erasure wherein a pre-flood channel network is mostly or totally obliterated.

The reduction of the stream-link area at the expense of bar formation is rapid during the approximately 10 years following the erasure event but appears to decrease beyond that. Large bars left in the wake of the extraordinary flood are dissected into smaller bars by subsequent flood events. This process increases the nodal density in the flood-modified channel. The confluence densities first increase around and downstream of narrow channel sections and tributary confluences, and this leads to a spatially uneven distribution of the resulting bars.

The geometric index of braiding reaches the pre-flood state the fastest, in approximately 15–24 years. However, about 25 years are required for the maximum junction-node density and stream-link area to reach the pre-flood situation. With additional time, the junction density and, accordingly, the braiding structures of stream-links and bars become more widely spread and uniformly distributed in the affected reaches within 30–35 years after the extreme flood event.

Despite some uncertainties, it proved possible to produce a decadal assessment of the fluviomorphic trajectories for the two ephemeral stream study sites, demonstrating that relatively simple geometric analytical methods can document the relevant processes for a data-scarce region. The results of this study could help estimate geomorphic recovery rates in the wake of extreme floods in dryland ephemeral channels with characteristics similar to our study sites. They may also help inform stream channel restoration and management efforts. Due to sparse observation networks in these arid regions, the observed recovery times and channel network changes presented here may help to assess recent occurrences of extreme flood events interpreted from timely aerial imagery and field inspection and approximate how much time has passed since the last occurrence of such a flood. Thus, the results can be applied for *approximating* aspects of regional flood histories in similar stream systems and also as baseline information to assess and detect the impacts of potential future increases in flood magnitude and frequency in this region.

DISCLAIMER

Any use of trade, firm or product names is for descriptive purposes only and does not imply endorsement by the US government.

AUTHOR CONTRIBUTIONS

Eliisa Lotsari: Conceptualization; funding acquisition; methodology; investigation; writing—original draft; writing—review and editing. **P. Kyle House:** Conceptualization; investigation; resources; writing—review and editing. **Petteri Alho:** Investigation; funding acquisition; writing—review and editing. **Victor R. Baker:** Resources; writing—review and editing.

ACKNOWLEDGEMENTS

The funding has been gained from the Academy of Finland (DefrostingRivers project, Grant Number 338480; ExRIVER project, Grant Number 267345; and RivCHANGE project, Grant Number 136234) and the University of Turku (Turun Yliopisto), Department of Geography and Geology (Geography section). We also thank Dr. Philip A. Pearthree from the Arizona Geological Survey for assisting in the field in March 2013 and for helping in gathering the aerial photographs from Bronco Creek. We thank Jin Li from the University of Arizona for helping to estimate and calculate the recurrence intervals of the extraordinary floods in Bronco Creek and Eldorado Canyon.

CONFLICT OF INTEREST STATEMENT

The authors have no conflicts of interest to declare.

DATA AVAILABILITY STATEMENT

The data applied are mostly open-access data. Freely downloadable aerial photographs from USGS EarthExplorer were applied (cf. Table 2). Unfortunately, due to third parties and multiple producers of the data, we are not able to open the rest of the datasets.

ORCID

Eliisa Lotsari https://orcid.org/0000-0002-0120-8722
Victor R. Baker https://orcid.org/0000-0002-4542-0469

REFERENCES

Adams, D.K. & Comrie, A.C. (1997) The North American monsoon. *Bulletin of the American Meteorological Society*, 78(10), 2197–2214. Available from: https://doi.org/10.1175/1520-0477(1997)078<2197:TNAM>2.0.CO;2

Aldridge, B.N. (1972) Investigation of floods from small drainage basins in Arizona. In: *Proceedings of the 21st Annual Conference on Roads and Streets*. Tucson, University of Arizona, Arizona Transportation and Traffic Institute, United States, pp. 107–126.

Aldridge, B.N. (1978) Unusual hydraulic phenomena of flash floods in Arizona. In: *Conference on flash floods—hydrometeorological aspects*. Boston: American Meteorological Society, pp. 117–120.

Bacon, S.N., Mcdonald, E.V., Caldwell, T.G. & Dalldorf, G.K. (2010) Timing and distribution of alluvial fan sedimentation in response to strengthening of late Holocene ENSO variability in the Sonoran Desert, Southwestern Arizona, USA. *Quaternary Research*, 73(3), 425–443. Available from: https://doi.org/10.1016/j.yqres.2010.01.004

Baker, V. (1977) Stream-channel response to floods, with examples from central Texas. *GSA Bulletin*, 88(8), 1057–1071. Available from: https://doi.org/10.1130/0016-7606(1977)88<1057:SRTFWE>2.0.CO;2

Billi, P., Demissie, B., Nyssen, J., Moges, G. & Fazzini, M. (2018) Meander hydromorphology of ephemeral streams: similarities and differences with perennial rivers. *Geomorphology*, 319, 35–46. Available from: https://doi.org/10.1016/j.geomorph.2018.07.003

Brierley, G.J. & Fryirs, K.A. (2016) The use of evolutionary trajectories to guide 'moving targets' in the management of river futures. *River Research and Applications*, 32(5), 823–835. Available from: https://doi.org/10.1002/rra.2930

Bull, W.B. (1997) Discontinuous ephemeral streams. *Geomorphology*, 19(3–4), 227–276. Available from: https://doi.org/10.1016/S0169-555X(97)00016-0

Bullard, K.L. (1986) Comparison of estimated maximum flood peaks with historic floods. US Bureau of Reclamation Technical Report.

Cadol, D., Rathburn, S.L. & Cooper, D.J. (2011) Aerial photographic analysis of channel narrowing and vegetation expansion in Canyon de Chelly National Monument, Arizona, USA, 1935–2004. *River Research and Applications*, 27(7), 841–856. Available from: https://doi.org/10.1002/rra.1399

Calle, M., Lotsari, E., Kukko, A., Alho, P., Kaartinen, H., Rodriguez-Lloveras, X., et al. (2015) Morphodynamics of an ephemeral gravel-bed stream combining Mobile Laser Scanner, hydraulic simulations and geomorphological indicators. *Zeitschrift für Geomorphologie*, 59(3), 33–57. Available from: https://doi.org/10.1127/zfg_suppl/2015/S-59196

Carmody, T. (1980) *A critical examination of the 'largest' floods in Arizona: a study to advance the methodology of assessing the vulnerability of bridges to floods for the Arizona Department of Transportation, General Report 1*. 53 pp. Tucson: Engineering Experimental Station, College of Engineering, University of Arizona.

Chew, L.C. & Ashmore, P.E. (2001) Channel adjustment and a test of rational regime theory in a proglacial braided stream. *Geomorphology*, 37(1–2), 43–63. Available from: https://doi.org/10.1016/S0169-555X(00)00062-3

Chin, A. & Gregory, K.J. (2001) Urbanization and adjustment of ephemeral stream channels. *Annals of the Association of American Geographers*, 91(4), 595–608. Available from: https://doi.org/10.1111/0004-5608.00260

Costa, J.E. (1987) A comparison of the largest rainfall-runoff floods in the United States with those of the People's Republic of China and the world. *Journal of Hydrology*, 96(1–4), 101–115. Available from: https://doi.org/10.1016/0022-1694(87)90146-6

Costa, J.E. & Jarrett, R.D. (2008) *An evaluation of selected extraordinary floods in the United States reported by the U.S. Geological Survey and implications for future advancement of flood science*, Scientific Investigations Report 2008-5164. US Department of the Interior, US Geological Survey, Reston, Virgina, United States.

de Musso, N.M., Capolongo, D., Caldara, M., Surian, N. & Pennetta, L. (2020) Channel changes and controlling factors over the past 150 years in the Basento River (southern Italy). *Watermark*, 12(1), 307. Available from: https://doi.org/10.3390/w12010307

East, A.E., Jenkins, K.J., Happe, P.J., Bountry, J.A., Beechie, T.J. & Mastin, M.C. (2017) Channel-planform evolution in four rivers of Olympic National Park, Washington, USA: the roles of physical drivers and trophic cascades. *Earth Surface Processes and Landforms*, 42(7), 1011–1032. Available from: https://doi.org/10.1002/esp.4048

East, A.E. & Sankey, J.B. (2020) Geomorphic and sedimentary effects of modern climate change: current and anticipated future conditions in the western United States. *Reviews of Geophysics*, 58(4), e2019RG000692. Available from: https://doi.org/10.1029/2019RG000692

Egozi, R. & Ashmore, P. (2008) Defining and measuring braiding intensity. *Earth Surface Processes and Landforms*, 33(14), 2121–2138. Available from: https://doi.org/10.1002/esp.1658

Enzel, Y., Ely, L.L., House, P.L., Baker, V.R. & Webb, R.H. (1993) Paleoflood evidence for a natural upper bound to flood magnitudes in the Colorado River Basin. *Water Resources Research*, 29(7), 2287–2297. Available from: https://doi.org/10.1029/93WR00411

Fowler, H.J., Lenderink, G., Prein, A.F., Westra, S., Allan, R.P., Ban, N., et al. (2021) Anthropogenic intensification of short-duration rainfall extremes. *Nature Reviews Earth and Environment*, 2(2), 107–122. Available from: https://doi.org/10.1038/s43017-020-00128-6

Friedman, J.M. & Lee, V.J. (2002) Extreme floods, channel change, and riparian forests along ephemeral streams. *Ecological Monographs*, 72(3), 409–425. Available from: https://doi.org/10.2307/3100097

Friend, P.F. & Sinha, R. (1993) Braiding and meandering parameters. In: Best, J.L. & Bristow, C.S. (Eds.) *Braided rivers*, Vol. 75. Geological Society, London, UK, Special Publication, pp. 105–111.

Gatewood, J.S., Schrader, F.F. & Stackpole, M.R. (1946) *Notable local floods of 1939*. United States Department of the Interior and Geological Survey. Water-Supply Paper 967, parts I-III, Washington: Unites States Government Printing Office 68 p.

Glancy, P.A. & Harmsen, L. (1975) *A hydrologic assessment of the September 14, 1974, flood in Eldorado Canyon, Nevada*, Geological Survey Professional Paper 930. Washington: United States Government Printing Office.

Graf, W.L. (1977) The rate law in fluvial geomorphology. *American Journal of Science*, 277(2), 178–191. Available from: https://doi.org/10.2475/ajs.277.2.178

Graf, W.L. (1981) Channel instability in a braided, sand bed river. *Water Resources Research*, 17(4), 1087–1094. Available from: https://doi.org/10.1029/WR017i004p01087

Graf, W.L. (1988) *Fluvial processes in dryland rivers*. New York: Springer-Verlag.

Gray, A.B. (2018) The impact of persistent dynamics on suspended sediment load estimation. *Geomorphology*, 322, 132–147. Available from: https://doi.org/10.1016/j.geomorph.2018.09.001

Hadley, R.F. (1968) Ephemeral streams. In: *Geomorphology. Encyclopedia of earth science*. Berlin, Heidelberg: Springer. https://doi.org/10.1007/3-540-31060-6_108

Hawkins, G.A., Vivoni, E.R., Robles-Morua, A., Mascaro, G., Rivera, E. & Dominguez, F. (2015) A climate change projection for summer hydrologic conditions in a semiarid watershed of central Arizona. *Journal of Arid Environments*, 118, 9–20. Available from: https://doi.org/10.1016/j.jaridenv.2015.02.022

Hjalmarson, H.W. & Phillips, J.V. (1997) Potential effects of translatory waves on estimation of peak flows. *Journal of Hydraulic Engineering*, 123(6), 571–575. Available from: https://doi.org/10.1061/(ASCE)0733-9429(1997)123:6(571)

Hooke, J.M. (2007) Monitoring morphological and vegetation changes and flow events in dryland river channels. *Environmental Monitoring and Assessment*, 127(1–3), 445–457. Available from: https://doi.org/10.1007/s10661-006-9294-6

Hooke, J.M. (2015) Variations in flood magnitude–effect relations and the implications for flood risk assessment and river management. *Geomorphology*, 251, 91–107. Available from: https://doi.org/10.1016/j.geomorph.2015.05.014

Hooke, J.M. (2016a) Morphological impacts of flow events of varying magnitude on ephemeral channels in a semiarid region. *Geomorphology*, 252, 128–143. Available from: https://doi.org/10.1016/j.geomorph.2015.07.014

Hooke, J.M. (2016b) Geomorphological impacts of an extreme flood in SE Spain. *Geomorphology*, 263, 19–38. Available from: https://doi.org/10.1016/j.geomorph.2016.03.021

Hooke, J.M. & Mant, J.M. (2000) Geomorphological impacts of a flood event on ephemeral channels in SE Spain. *Geomorphology*, 34(3–4), 163–180. Available from: https://doi.org/10.1016/S0169-555X(00)00005-2

House, P.K. & Baker, V.R. (2001) Paleohydrology of flash floods in small desert watersheds in western Arizona. *Water Resources Research*, 37(6), 1825–1839. Available from: https://doi.org/10.1029/2000WR900408

House, P.K. & Hirschboeck, K.K. (1997) Hydroclimatological and paleohydrological context of extreme winter flooding in Arizona, 1993. In: Larson, R.A. & Slosson, J.E. (Eds.) *Storm-induced geologic hazards: case histories from the 1992–1993 winter in Southern California and Arizona*, Reviews in Engineering Geology, Vol. 11. Boulder, CO: Geological Society of America, pp. 1–24.

House, P.K. & Pearthree, P.A. (1995) A geomorphologic and hydrologic evaluation of an extraordinary flood discharge estimate: Bronco Creek, Arizona. *Water Resources Research*, 31(12), 3059–3073. Available from: https://doi.org/10.1029/95WR02428

House, P.K., Pearthree, P.A. & Baker, V.R. (1998) Discussion and closure: potential effects of translatory waves on estimation of peak flows. *Journal of Hydraulic Engineering*, 124(11), 1178–1179. Available from: https://doi.org/10.1061/(ASCE)0733-9429(1998)124:11(1178)

Howard, A.D., Keetch, M.E. & Vincent, C.L. (1970) Topological and geometrical properties of braided streams. *Water Resources Research*, 6(6), 1674–1688. Available from: https://doi.org/10.1029/WR006i006p01674

Intergovernmental Panel on Climate Change. (2021) Summary for policymakers. In: Masson-Delmotte, V., Zhai, P., Pirani, A., Connors, S.L., Péan, C., Berger, S., *et al.* (Eds.) *Climate change 2021: the physical science basis. Contribution of Working Group I to the Sixth Assessment Report of the Intergovernmental Panel on Climate Change*. Cambridge University Press.

Jaeger, K.L. & Wohl, E. (2011) Channel response in a semiarid stream to removal of tamarisk and Russian olive. *Water Resources Research*, 47(2), W02563. Available from: https://doi.org/10.1029/2009WR008741

Jarrett, R.D. (1984) Hydraulics of high-gradient streams. *Journal of Hydraulic Engineering*, 110(11), 1519–1539.

Kampf, S.K., Faulconer, J., Shaw, J.R., Lefsky, M., Wagenbrenner, J.W. & Cooper, D.J. (2018) Rainfall thresholds for flow generation in desert ephemeral streams. *Water Resources Research*, 54(12), 9935–9950. Available from: https://doi.org/10.1029/2018WR023714

Kampf, S.K., Faulconer, J., Shaw, J.R., Sutfin, N.A. & Cooper, D.J. (2016) Rain and channel flow supplements to subsurface water beneath hyper-arid ephemeral stream channels. *Journal of Hydrology*, 536, 524–533. Available from: https://doi.org/10.1016/j.jhydrol.2016.03.016

Kidová, A., Lehotský, M. & Rusnák, M. (2016) Geomorphic diversity in the braided-wandering Belá River, Slovak Carpathians, as a response to flood variability and environmental changes. *Geomorphology*, 272, 137–149. Available from: https://doi.org/10.1016/j.geomorph.2016.01.002

Knox, J.C. (1972) Valley alluviation in southwestern Wisconsin. *Annals of the Association of American Geographers*, 62(3), 401–410. Available from: https://doi.org/10.1111/j.1467-8306.1972.tb00872.x

Kochel, R.C. (1988) Geomorphic impact of large floods: review and new perspectives on magnitude and frequency. In: Baker, V.R., Kochel, R.C. & Patton, P.C. (Eds.) *Flood geomorphology*. John Wiley & Sons, Inc., New York, United States, pp. 169–187.

Lotsari, E., Calle, M., Benito, G., Kukko, A., Kaartinen, H., Hyyppä, J., et al. (2018) Topographical change caused by moderate and small floods in a gravel bed ephemeral river—a depth-averaged morphodynamic simulation approach. *Earth Surface Dynamics*, 6(1), 163–185. Available from: https://doi.org/10.5194/esurf-6-163-2018

Mascaro, G. (2018) On the distributions of annual and seasonal daily rainfall extremes in central Arizona and their spatial variability. *Journal of Hydrology*, 559, 266–281. Available from: https://doi.org/10.1016/j.jhydrol.2018.02.011

Miall, A.D. (1977) A review of the braided-river depositional environment. *Earth-Science Reviews*, 13(1), 1–62. Available from: https://doi.org/10.1016/0012-8252(77)90055-1

Miller, D.M., Schmidt, K.M., Mahan, S.A., McGeehin, J.P., Owen, L.A., Barron, J.A., et al. (2010) Holocene landscape response to seasonality of storms in the Mojave Desert. *Quaternary International*, 215(1–2), 45–61. Available from: https://doi.org/10.1016/j.quaint.2009.10.001

National Oceanic and Atmospheric Administration. (2022) Data: daily summaries. https://www.ncei.noaa.gov/data/daily-summaries/access/Data

Ortega, J.A., Razola, L. & Garzón, G. (2014) Recent human impacts and change in dynamics and morphology of ephemeral rivers. *Natural Hazards and Earth System Sciences*, 14(3), 713–730. Available from: https://doi.org/10.5194/nhess-14-713-2014

Osterkamp, W.R. & Friedman, J.M. (2000) The disparity between extreme rainfall events and rare floods—with emphasis on the semi-arid American West. *Hydrological Processes*, 14(16–17), 2817–2829. Available from: https://doi.org/10.1002/1099-1085(200011/12)14:16/17<2817::AID-HYP121>3.0.CO;2-B

Paretti, N.V., Kennedy, J.R., Turney, L.A. & Veilleux, A.G. (2014) Methods for estimating magnitude and frequency of floods in Arizona, developed with unregulated and rural peak-flow data through water year 2010. US Geological Survey Scientific Investigations Report 2014-5211, 61 p. https://doi.org/10.3133/sir20145211

Parker, G. (1976) On the cause and characteristic scales of meandering and braiding in rivers. *Journal of Fluid Mechanics*, 76(03), 457–2480. Available from: https://doi.org/10.1017/S0022112076000748

Pascale, S., Carvalho, L., Adams, D.K., Castro, C.L. & Cavalcanti, I.F. (2019) Current and future variations of the monsoons of the Americas in a warming climate. *Current Climate Change Reports*, 5(3), 125–144. Available from: https://doi.org/10.1007/s40641-019-00135-w

Rinaldi, M., Bussettini, M., Surian, N., Comiti, F. & Gurnell, A.M. (2016) *Guidebook for the evaluation of stream morphological conditions by the Morphological Quality Index (MQI)*. ISPRA 177 pp.

Sanchis-Ibor, C., Segura-Beltrán, F. & Almonacid-Caballer, J. (2015) *Ephemeral rivers recovery under sediment and water deficit conditions. The case of Palancia River. II Congreso Ibérico de Restauración Fluvial—RESTAURARIOS 2015. Seminario final del Proyecto Life+ territorio vison, Pamplona—Navarra, 9–11 June, 2015*. Centro Ibérico de Restauración Fluvial, Spain, pp. 636–645.

Segura, C., Sun, G., McNulty, S. & Zhang, Y. (2014) Potential impacts of climate change on soil erosion vulnerability across the conterminous United States. *Journal of Soil and Water Conservation*, 69(2), 171–181. Available from: https://doi.org/10.2489/jswc.69.2.171

Sharon, D. (1972) The spottiness of rainfall in a desert area. *Journal of Hydrology*, 17(3), 161–175. Available from: https://doi.org/10.1016/0022-1694(72)90002-9

Smith, A., Sampson, C. & Bates, P. (2015) Regional flood frequency analysis at the global scale. *Water Resources Research*, 51(1), 539–553. Available from: https://doi.org/10.1002/2014WR015814

Smith, J.A., Baeck, M.L., Yang, L., Signell, J., Morin, E. & Goodrich, D.C. (2019) The paroxysmal precipitation of the desert: flash floods in the Southwestern United States. *Water Resources Research*, 55(12), 10218–10247. Available from: https://doi.org/10.1029/2019WR025480

Tellman, B., Sullivan, J.A., Kuhn, C., Kettner, A.J., Doyle, C.S., Brakenridge, G.R., et al. (2021) Satellite imaging reveals increased proportion of population exposed to floods. *Nature*, 596(7870), 80–86. Available from: https://doi.org/10.1038/s41586-021-03695-w

Tooth, S. (2000a) Downstream changes in dryland river channels: the Northern Plains of arid central Australia. *Geomorphology*, 34(1–2), 33–54. Available from: https://doi.org/10.1016/S0169-555X(99)00130-0

Tooth, S. (2000b) Process, form and change in dryland rivers: a review of recent research. *Earth-Science Reviews*, 51(1–4), 67–107. Available from: https://doi.org/10.1016/S0012-8252(00)00014-3

Tousi, E.G., O'Brien, W., Doulabian, S. & Toosi, A.S. (2021) Climate changes impact on stormwater infrastructure design in Tucson Arizona. *Sustainable Cities and Society*, 72, 103014. Available from: https://doi.org/10.1016/j.scs.2021.103014

United States Department of Agriculture, Soil Conservation Service. (1977) Flood hazard analyses, Las Vegas Wash and Tributaries, Clark County, Nevada. Special report: history of flooding, Clark County, Nevada, 1905–1975. Prepared in cooperation with Clark County Conservation District, Clark County Public Works Department, City of Las Vegas Public Works Department, City of North Las Vegas Public Works Department and Nevada Division of Water Resources. Las Vegas, Nevada, United States, 160 p.

US Geological Survey. (2016a) EarthExplorer. USGS Earth Resources Observation and Science Center (EROS) Archive. Aerial Photo Single Frames. Accessed during December 2016–April 2017 (https://earthexplorer.usgs.gov/). https://doi.org/10.5066/F7610XKM

US Geological Survey. (2016b) EarthExplorer. USGS Earth Resources Observation and Science Center (EROS) Archive. National High Altitude Photography (NHAP). Accessed during December 2016–April 2017 (https://earthexplorer.usgs.gov/). https://doi.org/10.5066/F7M043NG

US Geological Survey. (2016c) EarthExplorer. USGS Earth Resources Observation and Science Center (EROS) Archive. High Resolution Orthoimagery (HRO). Accessed during December 2016–April 2017 (https://earthexplorer.usgs.gov/). https://doi.org/10.5066/F73X84W6

US Geological Survey. (2016d) EarthExplorer. USGS Earth Resources Observation and Science Center (EROS) Archive. National Agriculture Imagery Program (NAIP). Accessed during December 2016–April 2017 (https://earthexplorer.usgs.gov/). https://doi.org/10.5066/F7QN651G

US Geological Survey. (2016e) EarthExplorer. USGS Earth Resources Observation and Science Center (EROS) Archive. Digital orthophoto quadrangle (DOQs). Accessed during December 2016–April 2017 (https://earthexplorer.usgs.gov/). https://doi.org/10.5066/F7125QVD

Wentworth, C.K. (1922) A scale of grade and class terms for clastic sediments. *The Journal of Geology*, 30, 377–392.

Western Regional Climate Center. (2011) Comparative data for Western states. Reno, Nevada, United States. https://wrcc.dri.edu/Climate/comp_tables_states_west.php

Wolman, M.G. & Gerson, R. (1978) Relative scales of time and effectiveness of climate in watershed geomorphology. *Earth Surface Processes and Landforms*, 3(2), 189–208. Available from: https://doi.org/10.1002/esp.3290030207

Wolman, M.G. & Miller, J.P. (1960) Magnitude and frequency of forces in geomorphic processes. *Journal of Geology*, 68(1), 54–74. Available from: https://doi.org/10.1086/626637

Zhang, Y., Hernandez, M., Anson, E., Nearing, M.A., Wei, H., Stone, J.J., et al. (2012) Modeling climate change effects on runoff and soil erosion in southeastern Arizona rangelands and implications for mitigation with conservation practices. *Journal of Soil and Water Conservation*, 67(5), 390–405. Available from: https://doi.org/10.2489/jswc.67.5.390

Ziaco, E., Miley, N. & Biondi, F. (2020) Reconstruction of seasonal and water-year precipitation anomalies from tree-ring records of the southwestern United States. *Palaeogeography, Palaeoclimatology, Palaeoecology*, 547, 109689. Available from: https://doi.org/10.1016/j.palaeo.2020.109689

Ziliani, L. & Surian, N. (2012) Evolutionary trajectory of channel morphology and controlling factors in a large gravel-bed river. *Geomorphology*, 173–174, 104–117. Available from: https://doi.org/10.1016/j.geomorph.2012.06.001

How to cite this article: Lotsari, E., House, P.K., Alho, P. & Baker, V.R. (2024) Fluviomorphic trajectories for dryland ephemeral stream channels following extreme flash floods. *Earth Surface Processes and Landforms*, 1–23. Available from: https://doi.org/10.1002/esp.5847